NASA Contractor Report 177938

NASA-CR-177938
19850024796

ON THE APPLICATION OF A HAIRPIN VORTEX MODEL OF WALL TURBULENCE TO TRAILING EDGE NOISE PREDICTION

N. S. LIU and S. J. SHAMROTH

SCIENTIFIC RESEARCH ASSOCIATES, INC.

GLASTONBURY, CT 06033

Contract NAS1—17249

August 1985

National Aeronautics and
Space Administration

Langley Research Center
Hampton, Virginia 23665

TABLE OF CONTENTS

SUMMARY

The goal of the present work is to develop a technique via a hairpin vortex model of the turbulent boundary layer, which would lead to the estimation of the aerodynamic input for use in trailing edge noise prediction theories. The work described herein represents an initial step in reaching this goal. The hairpin vortex is considered as the underlying structure of the wall turbulence and the turbulent boundary layer is viewed as an ensemble of typical hairpin vortices of different sizes. A synthesis technique is examined which links the mean flow and various turbulence quantities via these typical vortices. The distribution of turbulence quantities among vortices of different scales follows directly from the probability distribution needed to give the measured mean flow vorticity. The main features of individual representative hairpin vortices are discussed in detail and a preliminary assessment of the synthesis approach is made.

LIST OF SYMBOLS

Symbols

C	Strength factor of vortices or the effective centerline of a vortex filament
d	Distance between a point and the effective centerline of a vortex filament
e	Average streamwise spacing between representative vortices of the same hierarchy
f,g	General functional representations
h	Height of a vortex
l	Streamwise extent of the domain of significant influence of a hairpin vortex
p	Static pressure
P	Normalized probability distribution function of hierarchy of vortices
q	Convection velocity of a vortex
r	Linear correlation coefficient
Re_θ	Reynolds number based on momentum thickness
r_d	Decision point of the linear correlation
r_o	Effective radius of viscous core of a vortex filament
$\vec{r}$	Position vector
$\vec{r}_c$	Position vector of the effective centerline of a vortex filament
t	Time
U_m	Measured mean velocity
u,v,w	Cartesian velocity components
$\vec{v}$	Velocity vector
x,y,z	Cartesian coordinates
$\langle \cdot \rangle$	Averaged contribution due to the fluctuation field of a representative hairpin vortex

LIST OF SYMBOLS (Continued)

Greek Symbols

ε	Small parameter or error
Γ	Circulation
κ	Von Karman constant
λ	Average spanwise spacing of a hairpin vortex
ϕ	Characteristic angle of vortex
ν	Kinematic viscosity
ρ	Density
$\rho(h)$	Probability density function of h

Subscripts

i	Associated with the ith representative hairpin vortex or associated with the ith hierarchy of hairpin vortices
j	Associated with the jth vertical point
m	Measured mean value

Superscripts

+	Values evaluated in wall unit
~	Values measured in a coordinate system attached to the vortex
-	Expected mean value due to an ensemble of vortices

INTRODUCTION

Sound is produced when the wing or blade interacts with the unsteady flow structures generated by the wing's or blade's own motion. The noise production away from the trailing edge is due only to the evolution of these structures, and it is not an effective acoustic source. However, when these turbulent structures pass the trailing edge, the edge scatters the essentially nonpropagating flow fluctuations into a propagating sound field of dipole character. Thus, the noise due to the interactions between incident turbulence and trailing edge, i.e., the trailing edge noise, can make a significant contribution to the broadband sound field [1]. Recent experimental works in trailing edge noise have been focused upon the study of two-dimensional low Mach number turbulent flow over an airfoil (see e.g. [2] and [3]). A theoretical approach for predicting the far-field trailing edge noise characteristics is provided by evanescent wave theory (see e.g. [4]), or a related method due to Amiet (see, e.g. [5]). The required input to these methods is the incident surface pressure data obtained close to but sufficiently upstream of the edge and in the form of either the cross spectrum or the equivalent wave number spectrum. At the present time, these data are obtained mainly by extensive measurements. Thus, it is highly desirable to develop analytical techniques to provide these pertinent statistical quantities with a considerable saving in the amount of experimental works needed.

Determination of statistical characteristics of fluctuating surface pressure from first-principles fluid dynamic theory is not currently practical. The purpose of the present work is to investigate possible ways to relate the statistical properties of wall pressure fluctuations beneath turbulent boundary layers to the overall gross properties of the mean flows such that practically useful estimations of these statistical quantities can be obtained with a minimum amount of measurements. Pivotal to the achievement of such an objective is the use of a pertinent wall turbulence model to obtain a link between the mean flow and statistical properties of the wall pressure fluctuations. In the following, previous works about the models of wall turbulence structure will be briefly reviewed in the context of the estimation of certain statistical quantities of wall pressure.

Virtually all the published theoretical works on the subject of the statistical properties of the wall pressure fluctuations have been based upon the solution of the Poisson equation of pressure with non-linear fluctuating stress terms and terms involving interaction with the mean shear considered as source terms. Several assumptions about the form of these source terms are made and experimental information in regard to the fluctuating velocity field is used to estimate the root-mean-square wall pressure and, in some cases, the power spectrum of the wall pressure as well (see e.g. [6]). An alternate approach was suggested in [7] which represented shear flow turbulence as a random superposition of appropriate characteristic waves. More specifically, an attempt was made to relate the fluctuating pressures to the stability problem for the mean turbulent flow such that the cross-spectral density of the wall pressure might be estimated from the one-point power spectrum and the mean velocity distribution. This goal was partly reached. The possibility of modelling wall turbulence with waves also had been investigated in [8].

The present approach is different from previous efforts. In this approach the hairpin vortex is considered as the underlying structure of the wall turbulence and is used to link the mean flow with various statistical quantities of the fluctuating velocity and pressure fields. The present report focuses upon a preliminary assessment of the feasibility of using the hairpin-vortex concept to construct pertinent statistical quantities of turbulent boundary layer flows. In the following, various aspects associated with the application of hairpin-vortex concept to study the properties of turbulent boundary layer flows are discussed.

ANALYSIS

Hairpin Vortex as Structure of Wall Turbulence

The concept of modelling the turbulent boundary layer with a random array of hairpin vortices was first suggested by Theodorsen [9] in 1955 and has subsequently been considered by many other workers (see, e.g. [10]). These earlier proposals tended to be rather in the nature of intuitively appealing hypotheses, supported only indirectly by experimental evidence. However, very convincing evidence for the existence of these vortices has been reported over the past five years by a large number of investigators using different techniques to study various features associated with the underlying structures of wall turbulence. A comprehensive account of these results will not be given here, nevertheless, selected works are cited to indicate the current status of the knowledge of the structure of turbulent boundary layer.

Experiments of Head and Bandyopadhyay [11] have provided very strong support for the hairpin vortices as the dominant structures in turbulent boundary layers. Flow visualization studies of the zero pressure gradient turbulent boundary layer at Reynolds numbers up to $Re_\theta \approx 10^4$ have shown that a turbulent boundary layer consists of a forest of hairpin vortices which are undergoing a stretch motion under the influences of the self-induced field as well as the pre-existing mean shear field, these stretched hairpin vortices are substantially straight over a large portion of their length and inclined in the downstream direction at a characteristic angle of approximately 45° to the wall. The lateral dimensions of these vortices are suggested to follow the Kline scaling, while their length appears to be limited only by the thickness of the layer. There is considerable evidence that these vortices originate from the longitudinal vortex motions in, or very close to, the viscous sublayer.

Combining anemometry and flow visualization, Falco [12] established that all of the structural features of turbulent boundary layers, e.g., the sweep and ejection events, identified before by other investigators can be associated with the evolution of a so-called pocket flow module, in which a hairpin vortex is formed and then dominates the flow behavior over a time duration extending over at least half of the flow module's life time. In Ref. [13] Dinkelacker evaluated results compiled from several measurements of wall pressure fluctuations and suggested that an important part of the observed wall pressure

patterns might be manifestations of the existence of hairpin vortices in the turbulent boundary layer flow. Viets and his coworkers [14], motivated by the potential application of forced, unsteady vortex generation for the improvement of efficiency and performance of various aerodynamic devices, artificially generated vortex structures with scales greater than the scales of the boundary layer near the wall and experimentally investigated the evolution of these structures. It is interesting to note that, although the scales involved are entirely different from those occurring in previously mentioned works, the general geometry and deformation of the structures are quite similar to those of hairpin vortices.

The above experimental studies provide strong evidence for the existence of hairpin vortices as one of the dominant structures in wall-bounded turbulent flows, however, as limited by the nature of their sampling and identification techniques, a hairpin vortex has only been indirectly observed in a turbulent boundary layer; i.e., the response of the visual indicators to the velocity field is observed. In addition, the probe data are limited by the number of spatial points at which correlations are obtained and by the small number of different quantities that have been measured. These deficiencies have largely been eliminated by a very recent investigation conducted by Moin and Kim [15] using a data base generated by the large-eddy simulation calculations. Two-point correlations of velocity and vorticity fluctuations strongly support a flow model consisting of vortical structures inclined at 45° to the wall. The instantaneous vorticity vectors plotted in these inclined planes show that the flow contains a large number of hairpin vortices, and vortex lines are used to display the three-dimensional structure of hairpins.

In another investigation Landahl [16] modelled the dominant coherent structure near the wall with a flat eddy, which can be regarded as a first approximation to the hairpin vortex, and then examined the fundamental assumptions behind Prandtl's mixing length theory. The validity of two of the main hypotheses underlying the mixing length theory has been positively confirmed. Thus, this work provides an encouraging indication of the consistency of over all fluid dynamics according to the conventional mixing length model and that due to the hairpin vortex.

As mentioned before, early turbulence models based on the concept of hairpin vortex tended to be in the nature of intuitively appealing hypotheses and were mainly aimed at providing a kinematic description of the wall

turbulence, as well as an explanation of some of the underlying dynamics. In the light of recent findings from experimental research on turbulent structures in the near wall region and also by using Townsend's attached-eddy hypothesis [17], Perry and his coworkers ([18], [19]) proposed a more refined hairpin vortex model for wall turbulence. The turbulent boundary layers are viewed as an ensemble of groups (or hierarchies) of hairpin vortices which originate from and are attached to the wall. These vortices are geometrically similar and have the same characteristic velocity scale being the wall shear velocity. The length scales of the hierarchies range from the smallest eddies having the Kline scaling to the largest eddies being of the order of the boundary layer thickness. The probability distribution for hierarchies is inversely proportional to the length scales of the hierarchies, and all the vortices lean 45° in the downstream direction. It is found that such a model gives the correct mean flow vorticity distribution. Further, by using the velocity signatures generated by hairpin vortex with the aid of the Biot-Savart law, turbulence spectral distributions are derived and, when compared with experimental results, the predicted turbulence spectra appear to have correct properties. Thus, in spite of the fact that there still exists uncertainties about the details of the formation, shape and subsequent evolution of the hierarchies of vortices, the works of Perry and his coworkers demonstrated that the use of hairpin vortices in obtaining a quantitative link between the mean flow, Reynolds shear stress, turbulence intensities and spectra as well as other statistical properties of wall turbulence looks quite promising.

Aspects of the Application of Hairpin Vortex Model of Turbulence

Under the premise that a mathematically operational model of hairpin vortex can be constructed (see e.g. the following section), the hairpin vortex can be used in different contexts to study various aspects associated with turbulent boundary layer flows. For example, the turbulent boundary layer might be simulated by an appropriate ensemble of hairpin vortices, then the dynamics of these vortices could be tracked either in Lagrangian reference frames by methods described in [20] or in an Eulerian reference frame by using continuity and momentum equations. However, at the present stage of the development of the hairpin vortex concept, it is felt that more fruitful insights could be obtained by pursuing in the directions of two distinct but

related approaches, namely, (i) the investigation of the dynamics of one or several separated representative hairpin vortices submerged in various background boundary layer flows which can be laminar or turbulent, with or without pressure gradients, and (ii) the construction of useful statistical models using hairpin vortices to provide a quantitative link between mean flow properties and turbulence properties. The latter approach is a synthesis approach and therefore is inherently kinematic in its nature, the dynamic informations are indirectly included through the specifications of the structural parameters of the modelling vortices. Obviously, these two approaches are complementary with each other, the experiences gained in one approach can be used to advance the other's development.

The present work focuses upon the construction of a model of hairpin vortices as well as the development of a statistical approach using a synthesis of these hairpin vortices to obtain estimations of turbulence transport properties. These items will be discussed in later sections. Here, some comments about the forms of the governing equations appropriate to the investigation of the evolution of hairpin vortices will be made.

Although the background flows can be considered as nominally steady and two-dimensional, the flow field associated with the evolving hairpin vortex is unsteady and three-dimensional, i.e., they are accompanied by negative cross flows and possible streamwise reverse flows. Thus, governing equations derived from conventional boundary layer theory are not suitable for the purpose of studying the dynamics of hairpin vortex. An approximate form of the unsteady three-dimensional Navier-Stokes equations has been used to solve the three-dimensional time-dependent viscous flows over airfoil sections [21]. These equations are more general than the conventional boundary layer equations, notably in the inclusion of spanwise and streamwise diffusion terms, and the major assumption is that there is no pressure gradient in the direction normal to the wall. The solution of this set of governing equations is less demanding in computer resources than the solution of the full Navier-Stokes equations. Unfortunately, the assumption of zero normal pressure gradient which is inherent in this extended boundary layer approach makes it inapplicable to the present investigation. In this regard it should be noted that, associated with the presence of a hairpin vortex, there exists a corresponding three-dimensional pressure field. Further, in the proximity of

the vortex, the pressure variations in all directions must be significant, unless the strength of the vortex is infinitesimal. In this sense, the existence of a hairpin vortex can be thought of as being sustained by a pressure field containing localized regions of significant gradients in all directions. The assumption that the normal pressure gradient is negligibly small throughout the entire flow field is thus contradictory to the presence of the hairpin vortex. In the following, the governing equations for the leading behavior of a vortex point in a background rotational flow field is derived by using the procedure described in [22]. This serves the dual purpose of demonstrating the role of pressure gradients as well as some dominant factors to be expected in the investigation of vortex dynamics.

Considering an initial vorticity distribution $\zeta(x,y,o)$ which consists of two parts:

$$\zeta(x,y,0) = f_1(x,y) + f_2(\tilde{x},\tilde{y}) \tag{1}$$

f_1 is the initial vorticity of the background rotational flow. It is distributed with the characteristic length scale L and its magnitude is of the order of U/L, where U is the characteristic velocity of the background flow. The portion f_2 represents a concentrated distribution near a point C(X(0),Y(0)) and it is of compact support or decays exponentially in $\tilde{r}$ where $\tilde{r}$ is the distance from C on a small length scale ϵL. Note that f_2 is a function of the stretched variables $\tilde{x}$ and $\tilde{y}$ with

$$\tilde{x} = \left[x - X(t)\right]/\epsilon\,, \qquad \tilde{y} = \left[y - Y(t)\right]/\epsilon \tag{2}$$

where (X(t), Y(t)) is the location of the vortex center and ϵ is a small parameter to be chosen. The total strength of f_2 is assumed to be of the order of UL, i.e.

$$\iint_{-\infty}^{\infty} f_2\,dx\,dy = \Gamma = O(UL) \tag{3}$$

Therefore

$$f_2 = \epsilon^{-2}\tilde{f}_2 \quad \text{with} \quad \tilde{f}_2 = O(1) \tag{4}$$

i.e.
$$\zeta(x, y, 0) = f_1(x, y) + \epsilon^{-2}\tilde{f}_2(\tilde{x}, \tilde{y}) \tag{5}$$

To take into account the viscous effects inside the core, ϵ is chosen as

$$\epsilon = \frac{1}{\sqrt{Re}} = \sqrt{\frac{\nu}{\Gamma}} \ll 1 \tag{6}$$

where Re is the Reynolds number, ν the kinematic viscosity and Γ the circulation. The assumption that $\Gamma=O(UL)$ is consistent with the hairpin vortex being a nonlinear, large scale structure in the wall region of the boundary layer flow. L is considered here as the boundary layer thickness and U being the wall frictional velocity.

Solutions of the unsteady Navier-Stokes equations with large Reynolds number subjected to the initial condition of Eq. (5) and appropriate boundary conditions are to be sought. The form of the initial data suggests that the solution is a composite of multiple length scales solutions:

$$\zeta(x, y, t; \epsilon) = \zeta_1(x, y, t; \epsilon) + \epsilon^{-2}\tilde{\zeta}_2(\tilde{x}, \tilde{y}, t; \epsilon) \tag{7}$$

such that at t=0

$$\zeta_1 = f_1(x, y) \quad \text{and} \quad \tilde{\zeta}_2 = \tilde{f}_2(\tilde{x}, \tilde{y})$$

Accordingly, the velocity and pressure are expressed as

$$u(x, y, t; \epsilon) = u_1(x, y, t; \epsilon) + \epsilon^{-1}\tilde{u}_2(\tilde{x}, \tilde{y}, t; \epsilon) \tag{8}$$

$$v(x, y, t; \epsilon) = v_1(x, y, t; \epsilon) + \epsilon^{-1}\tilde{v}_2(\tilde{x}, \tilde{y}, t; \epsilon) \tag{9}$$

$$p(x, y, t; \epsilon) = p_1(x, y, t; \epsilon) + \tilde{p}_{12}(\tilde{x}, \tilde{y}, t; \epsilon) + \epsilon^{-1}\tilde{p}_{21}(\tilde{x}, \tilde{y}, t; \epsilon) + \epsilon^{-2}\tilde{p}_2(\tilde{x}, \tilde{y}, t; \epsilon) \tag{10}$$

Substituting Eqs. (8)-(10) into the continuity and Navier-Stokes equations, it can be shown that the vorticity of the background flow is redistributed by the presence of the vortical structure while the dynamics of the vortical spot is controlled by several mechanisms. The most dominant mechanism is the self-induction, followed by the relative yet coupled motion between the vortex center and the local background flow; the effects of the temporal change of the structure and viscous diffusion are the least dominant ones. More specifically, with respect to an observer moving with the vortex center, the leading behavior of the evolution of the vortical spot is governed by the following equations:

$$\frac{\partial \tilde{u}_2^{(0)}}{\partial \tilde{x}} + \frac{\partial \tilde{v}_2^{(0)}}{\partial \tilde{y}} = 0 \tag{11}$$

$$\tilde{u}_2^{(0)} \frac{\partial \tilde{u}_2^{(0)}}{\partial \tilde{x}} + \tilde{v}_2^{(0)} \frac{\partial \tilde{u}_2^{(0)}}{\partial \tilde{y}} = -\frac{\partial \tilde{p}_2^{(0)}}{\partial \tilde{x}} \tag{12}$$

$$\tilde{u}_2^{(0)} \frac{\partial \tilde{v}_2^{(0)}}{\partial \tilde{x}} + \tilde{v}_2^{(0)} \frac{\partial \tilde{v}_2^{(0)}}{\partial \tilde{y}} = -\frac{\partial \tilde{p}_2^{(0)}}{\partial \tilde{y}} \tag{13}$$

where $\tilde{u}_2(0)$, $\tilde{v}_2(0)$ and $\tilde{p}_2(0)$ are the leading term of $\tilde{u}_2$, $\tilde{v}_2$ and $\tilde{p}_2$ when expanded into a power series of ε.

In view of equations (11)-(13), it is obvious that any flow simulation technique based on the assumption of zero normal pressure gradient throughout the entire flow field will immediately force a disintegration of the vortical structure, consequently, the general behavior of this structure cannot be properly studied. Based on this asymptotic analysis as well as the previously discussed physical manifestation of the existence of a concentrated vortical structure in terms of its associated pressure field, it is concluded here that Navier-Stokes equations should be used in the investigation of the dynamics of

hairpin vortices. Numerical techniques for the solution of unsteady, three-dimensional Navier-Stokes equations are currently available (see e.g. [23], [24]).

The above analysis indicates that the dominant behavior of the evolution of a vortical spot is governed by steady, Euler equations written in a coordinate system attached to the vortex center. Obviously, information about the motion of the vortex center, the interactions between the vortical spot and the surrounding background flow as well as the inner strucure of the vortical spot cannot be determined by these set of leading order equations. Such information must be obtained by investigating higher order equations derived in the asymptotic analysis. Generally speaking, the motion of the center of a two-dimensional vortical spot depends on its inner structure and the local background flow situation. For the three-dimensional case, the motion of the centerline of a vortex filament further depends on the geometrical properties of the centerline.

Another interesting consequence of the above asymptotic analysis is that the frequently employed Taylor's hypothesis of frozen eddies is a valid approximation to the leading order. Hence, if the position and the associated induced velocity field of a vortical structure is known at some instant, then the dominant part of the associated pressure field can be obtained by considering the steady, Euler equations. Subsequently, these velocity and pressure patterns may be considered as frozen over a certain time interval while convected by the background flow field. This frozen-eddy approximation will be used later for estimating the pressure field associated with a representative hairpin vortex and for the construction of a statistical model of turbulent boundary layer with the aid of hairpin vortices.

A Model of the Hairpin Vortex

As shown in Ref. [15], a hairpin vortex is an agglomeration of vortex lines in a compact region that have a hairpin or horseshoe shape (Fig. 1). Equivalently, a hairpin vortex is considered here as a slender tube-like region in which the bulk of vorticity is concentrated. Over each cross-section of this tube-like region, a mean direction, $\vec{e}_s$, as well as the strength, Γ, of the concentrated vorticity can be determined. Further, inside of this compact region, a spatial curve can be found such that its tangent is parallel to $\vec{e}_s$

boundary layer will not be included in the model. Thus, the present work focuses upon a hairpin vortex model most pertinent to the flow in the logarithmic law region. In addition, it is assumed that the hairpin vortices appear mostly in the form of an array in the spanwise direction, and members of the same array of vortices have identical properties. Such an assumption implies that the hairpin vortices are produced by the evolution of an initially spanwise-oriented two-dimensional vortex line into a three-dimensional wavy structure which is periodic in the spanwise direction.

Based on the above discussions, the fundamental hairpin vortex model used in the present work consists of a spanwise array of identical vortices. The effective centerline of these vortices forms an array of interconnecting isosceles triangles which are periodic in the spanwise direction. The strength of these vortices does not vary along the effective centerline which inclines to the wall at an angle of 45°. In order to maintain the attachment of these vortices to the rigid wall, their wall images are also included. The effects of the inner core structure of these vortices are accounted for by introducing a diffusive factor into the evaluation of the associated induced velocity field. A schematic of the present model is shown in Fig. 2, where h_i is the height of the i-th array of hairpin vortices, λ_i the spanwise distance between the feet of the vortices, $\phi_i = \phi = 45°$ the characteristic angle and r_{oi} the radius of the effective core. The signature or the induced velocity field of the i-th array of hairpin vortices at a point P with position vector $\vec{r}$ is then given by

$$\vec{v}_i(\vec{r}) = f_i(d_i, r_{oi}) \left[-\frac{\Gamma_i}{4\pi} \int_{c_i} \frac{(\vec{r}_{c_i} - \vec{r})}{|\vec{r}_{c_i} - \vec{r}|^3} \times d\vec{s}_i \right] \tag{16}$$

with

$$f_i(d_i, r_{oi}) = \frac{d_i^2}{d_i^2 + r_{oi}^2} \tag{17}$$

where C_i is the effective centerline of the vortices together with their wall images, and $d_i = \left|\vec{r}_{ci} - \vec{r}\right|$. The corresponding vorticity distribution is obtained from

$$\vec{\Omega}_i = \nabla \times \vec{v}_i \tag{18}$$

Obviously, when the array contains a sufficiently large number of vortices, the induced velocity field $\vec{v}_i$ and hence $\vec{\Omega}_i$ are periodic functions with spatial period λ_i. Therefore the induced field due to such an array of vortices is completely defined by the flow field within the spanwise domain of any one member of the vortices. Henceforth, the term 'representative' hairpin vortex will be used to indicate some particular member of the vortex array such that the point P happens to locate within the spanwise domain of this particular vortex (see Fig. 2). It should be noted that the induced flow field within a representative hairpin vortex contains not only the contribution of this vortex but also contains the contributions of all the other vortices in the same array.

The flow patterns within a representative hairpin vortex are shown from Fig. 3 to Fig. 6. These results are obtained by placing 31 vortices on each side of the representative vortex. This number of vortices gives an excellent approximation to the spanwise periodicity required by an infinite number of spanwise vortices. The velocity vector field and the region of spanwise vorticity concentration in planes parallel to the mean flow direction are given in Figs. 3 and 4. Figure 3 depicts the flow pattern at one foot of the representative hairpin vortex while Fig. 4 illustrates the pattern occurring at the tip of the vortex. The velocity vector field and the concentration region of normal vorticity component are shown in Figs. 5 and 6. Figure 5 indicates the pattern in a plane parallel to the flat wall and this plane is near the tip of the vortex. There apparently exists a pair of counter-rotating vortices of equal strengths. Similar pattern occurs at a plane closer to the wall, as illustrated by Fig. 6. In addition, Figs. 3 and 4 indicate that the induced field falls off rapidly in regions relatively away from the representative vortex. The vertical extent of the domain of significant influence of the representative vortex is approximately equal to h_i, its streamwise extent is of the order of $l_i = h_i \cot \phi_i$, while its spanwise extent remains to be of the order of λ_i.

Scaling and Main Features of the Hairpin Vortex Model

In the previous section, the general configuration and structure of a representative hairpin vortex have been presented. Since the turbulent boundary layer is viewed as an ensemble of representative hairpin vortices of different scales, it is necessary to provide a relationship between these representative vortices. Following the suggestions given in [18], it is assumed here that these representative hairpin vortices are geometrically similar and have the same characteristic veloicty scale. Consequently, the circulation of these vortices is proportional to their length scale, and the information regarding some 'baseline' representative vortex is needed for constructing an ensemble of vortices.

In the wall region, the properties of the vortices should scale with the wall unit. Let τ_w, u_τ and ν be the wall shear stress, frictional velocity and kinematic viscosity of the local mean flow, then the characteristic length, velocity, pressure and time of the vortex in the near wall region scale with the local ν/u_τ, u_τ, τ_w and ν/u_τ^2 respectively. In addition, the circulation is scaled with ν. It has been experimentally observed that the large scale structures in the near wall region have an averaged spanwise spacing of the order of 100 ν/u_τ [11] and an averaged streamwise spacing of the order of 440 ν/u_τ [26]. Based on these experimentally observed values and also by following the suggestions given in [18], the baseline vortex used in the present work has the following configurational and structural parameters:

$$\phi = 45° \tag{19}$$

$$\lambda^+ = 100 \tag{20}$$

$$h^+ = \frac{1}{2}\lambda^+ = 50 \tag{21}$$

$$r_o^+ = \frac{1}{20}\lambda^+ = 5 \tag{22}$$

$$e^+ = 4\lambda^+ = 400 \tag{23}$$

$$\Gamma^+ = \frac{c}{\kappa} e^+ = c \cdot 1000 \tag{24}$$

where the superscript '+' indicates that the quantities are evaluated in terms of wall unit and κ is the von Karman constant (κ=0.40). The strength factor C is a constant for a given ensemble of vortices; its specific value is determined along with the probability distribution of the vortices in a given ensemble (see the following section). Generally speaking, C is of the order of 1 and is assumed to be 1 at the present stage.

With this proposed baseline vortex as well as the assumed geometrical similarity between vortices, the induced velocity field associated with each member of the ensemble of representative vortices can be determined by first specifying its height and then applying Eq. (16). Since the present vortex model is expected to be most pertinent to the flow in the logarithmic law region, the heights of the vortices considered range from 100 ν/u_τ to 0.14δ where δ is the local boundary layer thickness.

The above analysis links the kinematic aspect of the hairpin vortices to the local mean flow properties. So far as their dynamic aspect is concerned, the present work for this initial effort assumes that, as a vortex passes by a local ground fixed point, its configuration as well as its structure are temporarily frozen and it is carried by the environment with a constant mean convection velocity in the downstream direction. This assumption implies that fluctuations observed at a local ground fixed point are due primarily to the passage of a vortex rather than the time rate of change of the vortex itself. Obviously, the mean convection velocity of the vortex cannot be completely determined by its own kinematic properties, a way to obtain the mean convection velocity of the hairpin vortex will be discussed later in this section. It is noted here that consideration of vortex decay and distortion effects could be included at a later date. These could be based upon experimental correlations or based upon Navier-Stokes calculations of the vortex distortion process.

Similarly, vortex convection velocity also could be estimated based upon a Navier-Stokes simulation. In the following, the main features of the frozen hairpin vortices are discussed. Let (x,y,z) be a coordinate system fixed on the ground and $(\tilde{x},\tilde{y},\tilde{z})$ be a coordinate system attached to some nominal center of the vortex under consideration. With respect to the ground fixed system and at some instant considered as $t=0$, the nominal vortex center is located at (x_o,o,z_o) and is translating in the x direction with a constant velocity q. Since the induced velocity field of the vortex is obtained with Biot-Savart integral, this field is evaluated with respect to the coordinate system $(\tilde{x},\tilde{y},\tilde{z})$. Let (u,v,w,p) denote the Cartesian velocity components and the pressure observed in (x,y,z) system and $(\tilde{u},\tilde{v},\tilde{w},\tilde{p})$ the corresponding quantities evaluated in $(\tilde{x},\tilde{y},\tilde{z})$ system, the frozen vortex assumption yields

$$u(x,y,z,t) = \tilde{u}(\tilde{x},\tilde{y},\tilde{z}) + q \tag{25}$$

$$v(x,y,z,t) = \tilde{v}(\tilde{x},\tilde{y},\tilde{z}) \tag{26}$$

$$w(x,y,z,t) = \tilde{w}(\tilde{x},\tilde{y},\tilde{z}) \tag{27}$$

$$p(x,y,z,t) = \tilde{p}(\tilde{x},\tilde{y},\tilde{z}) \tag{28}$$

with

$$x = \tilde{x} + qt + x_o \tag{29}$$

$$y = \tilde{y} \tag{30}$$

$$z = \tilde{z} + z_o \tag{31}$$

As mentioned above, the induced velocity components $\tilde{u}$, $\tilde{v}$ and $\tilde{w}$ are obtained with Biot-Savart integral, the determination of the associated pressure field is now discussed. Although the pressure is usually obtained by solving a Poisson equation subject to Neumann type boundary conditions, it is noted here that the assumption of frozen vortex convecting at a constant velocity leads to the following form of the normal momentum equation:

$$\tilde{u}\frac{\partial\tilde{v}}{\partial\tilde{x}} + \tilde{v}\frac{\partial\tilde{v}}{\partial\tilde{y}} + \tilde{w}\frac{\partial\tilde{v}}{\partial\tilde{z}} = -\frac{1}{\rho}\frac{\partial\tilde{p}}{\partial\tilde{y}} + \upsilon\tilde{\nabla}^2\tilde{v} \tag{32}$$

Accordingly,

$$\tilde{p}(\tilde{x},\tilde{y},\tilde{z}) = \tilde{p}_\infty(\tilde{x},\tilde{z}) + \rho\int_{\tilde{y}}^{\infty}\left[\tilde{u}\frac{\partial\tilde{v}}{\partial\tilde{x}} + \tilde{v}\frac{\partial\tilde{v}}{\partial\tilde{y}} + \tilde{w}\frac{\partial\tilde{v}}{\partial\tilde{z}} - \nu\tilde{\nabla}^2\tilde{v}\right]d\tilde{y} \tag{33}$$

Since the effect of the induced field falls off rapidly in regions outside the domain of significant influence of the vortex (see Fig. 4), $\tilde{p}_\infty(\tilde{x},\tilde{z})$ is considered here as uniformly and negligibly small.

The above discussions deal with the characteristics of the fluctuating velocity and pressure fields associated with the hairpin vortex model used in the present work. In this model, the configuration and structure of some baseline vortex is specified. With the assumption that representative vortices are geometrically similar, the configuration and structure of any other vortex can be determined by knowing its height. Consequently, its induced velocity field is obtained from evaluating the Biot-Savart integral in a coordinate system attached to the nominal center of the vortex. The additional assumption that the vortex is frozen while convecting at a constant velocity allows the induced pressure field to be determined by integrating the normal momentum equation written in a coordinate system attached to the nominal vortex center. This assumption also provides a connection between the apparent fluctuating flow field detected by a ground fixed observer and the induced flow field associated with a convecting vortex. The parameters involved in this mapping procedure are the relative position between the ground fixed observer and the

translating vortex center. When vortices are ensembled to represent a turbulent boundary layer, the heights of the vortices as well as the relative positions of the vortex centers with respect to a ground fixed observer are considered as random variables so that a statistical model of wall turbulence can be constructed. At this point, it becomes necessary to investigate the features of the mean flow field associated with the proposed hairpin vortex model.

Let $< u(y) >$ denote the contribution of one representative vortex to the total mean flow velocity measured by an observer located at fixed x and z. By virtue of Eqs. (25) and (29)-(31), the time-average of u-signals is transformed into the streamwise-average of $\tilde{u}$. In addition, with respect to the center of a representative vortex, the lateral position of the observer is a random point, it is assumed here that the probabilities of the observer being in the interval $-\lambda/2 \leq \tilde{z} \leq \lambda/2$ are equally likely, thus

$$<u(y)> = \frac{1}{\lambda}\frac{1}{e}\int_{-\frac{e}{2}}^{\frac{e}{2}}\int_{-\frac{\lambda}{2}}^{\frac{\lambda}{2}} \tilde{u}(\tilde{x},\tilde{y},\tilde{z})\,d\tilde{z}\,d\tilde{x} + q \tag{34}$$

where λ is the spanwise spacing of the vortices, e is the streamwise spacing of the vortices and the vortex center is at $(\tilde{x},\tilde{y},\tilde{z})=(0,0,0)$. Similar consideration yields

$$<f(y)> = \frac{1}{\lambda}\frac{1}{e}\int_{-\frac{e}{2}}^{\frac{e}{2}}\int_{-\frac{\lambda}{2}}^{\frac{\lambda}{2}} \tilde{f}(\tilde{x},\tilde{y},\tilde{z})\,d\tilde{z}\,d\tilde{x} \tag{35}$$

where f represents v, w, or p.

In the following, the fluctuation as well as the mean field of the baseline hairpin vortex are presented. The structural parameters are given in Eqs. (19)-(24) with C=1.0. Note that the streamwise velocity component $\tilde{u}^+$, the normal velocity component $\tilde{v}^+$ and the pressure $\tilde{p}^+$ are symmetrical about the center plane $\tilde{z}^+=0$ while the spanwise velocity component $\tilde{w}^+$ is antisymmetric about $\tilde{z}^+=0$. Therefore, it is sufficient to illustrate their spanwise variations by presenting the distributions on one side of the center plane. The variations in the normal direction are illustated by comparing the

distributions plotted at three horizontal planes with $y^+/h^+ = 0.4$, 0.8 and 1.6 respectively (Figs. 7-10). It is noted here that, when the pressure fluctuations are evaluated, the induced pressure at $y^+ = 400 = 8h^+$ is considered as zero. Fig. 10(c) shows that the induced pressure practically falls off to zero at $y^+ = 1.6h^+$. The results presented in Figs. 7-10 indicate that, depending upon the relative position between a ground fixed probe and some particular representative vortex which is passing by, the probe can pick up apparently different signals originating from the same vortex, these signals can be different in shape, in magnitude and in sign. Thus, when their relative positions become random, a ground fixed probe will then pick up an ensemble of apparently random fluctuating signals as a train of representative hairpin vortices passing by, even if these representative vortices are identical in their configuration and structure.

The mean flow field associated with the baseline hairpin vortex is illustrated in Fig. 11. It is noted that $< w^+ > = 0$ and $< v^+ >$ is one order of magnitude smaller than $< u^+ > - q^+$ which is the averaged value of the induced streamwise velocity of the vortex (see Eq. (34)). Figure 11(d) shows that the magnitude of the averaged fluctuating wall pressure due to the baseline representative vortex is about $2.3\tau_w$. Previous investigations on the rms wall pressure (see e.g. [6] and [27]) suggested that most of the wall-pressure-producing disturbances arise in the constant Reynolds shear stress region and the ratio of rms wall pressure to wall shear stress is between 1.7 and 3. Thus, the averaged wall pressure associated with the baseline vortex which locates fairly close to the constant Reynolds shear stress region seems to be in the right range of magnitude.

Figure 11(a) indicates that there exists a point y_*^+ at which the averaged value of the induced streamwise velocity vanishes. This point is slightly lower than, but quite close to the tip of the vortex. Obviously, for a ground fixed probe located at y_*^+, the measured mean flow velocity does not contain the contribution of the representative vortex under consideration. Whatever the measured mean value may be, it is due entirely to the environment which carries this particular vortex. Accordingly, the mean convection velocity of a representative hairpin vortex is defined here as the total mean flow velocity measured by a ground fixed probe placed at some particular point, at which the averaged value of the induced streamwise velocity of the hairpin vortex under

consideration vanishes. The averaged effects of a representative hairpin vortex on its surroundings are also illustrated by Fig. 11(a). In the region below the tip of the vortex, the presence of a train of representative vortices introduces a velocity defect to the pre-existing mean flow of the surroundings, while in the region above the tip of the vortex, they apparently introduce a velocity surplus to the surrounding mean flow. This can be viewed as an energy exchange between the hairpin vortices and their environment, namely, in the region characterized by $y^+ \leq h^+$, the vortices draw energy from the local, pre-existing mean flow, while in the region $y^+ > h^+$, the pre-existing mean flow velocity is increased due to the presence of these vortices.

The averaged streamwise induced velocity due to hairpin vortices of different sizes are shown in Fig. 12. Without the existence of a turbulent boundary layer, i.e., an ensemble of these hairpin vortices, the flow over a flat plate would be uniform everywhere, and is termed as the background flow in the following discussion. The presence of any one of these vortices will slightly increase the background flow velocity in a region which is above the vortex, this is equivalent to the entrainment effect. On the other hand, due to the vortex of $h^+ = 500$, an apparent velocity defect of the background flow is induced in the region $y^+ < 500$. This is interpreted here as a part of the background flow energy being consumed to sustain the existence of the vortex of $h^+ = 500$ so that a modified, new mean velocity profile now exists for the region $y^+ < 500$. Further, such a mean velocity profile again will be changed in the region $y^+ < 300$ to sustain the existence of a vortex of $h^+ = 300$. This cascade process is then continued for successively smaller vortices to produce successively reduced mean flow velocity as the wall is approached.

Figure 13 shows the averaged streamwise induced velocity of a representative hairpin vortex ($h^+ = 300$) in the semi-logarithmic form. It is clear that $< u^+ > - q^+$ is proportional to $\ln y^+$ over a substantial region of the vortex ($120 \leq y^+ \leq 280$). This indicates that the present hairpin vortex model is consistent with the observed mean flow behavior in the logarithmic law region. The averaged spanwise induced vorticities of various representative hairpin vortices are presented in Fig. 11(b) and Fig. 14. The following formula may be used to approximate the calculated $\partial <u^+> / \partial y^+$:

$$\frac{\partial \langle u^+ \rangle}{\partial y^+} \approx \begin{cases} \omega_o^+ & , \ y^+/h^+ < 0.8 \\ \omega_o^+ \left[1 - \frac{1}{0.4} (y^+/h^+ - 0.8) \right] & , \ 0.8 \leq y^+/h^+ \leq 1.2 \\ 0 & , \ y^+/h^+ > 1.2 \end{cases} \tag{36}$$

where ω_o^+ is a function of h^+ only and $d\omega_o^+/dh^+ < 0$.

These results also indicate that the contribution of a representative hairpin vortex to the mean flow vorticity diminishes quickly in the region beyond the height of the vortex and the contribution of larger vortices to the mean flow vorticity in the near wall region is far less significant than the contribution of smaller vortices (Fig. 14). Generally speaking, at a given level y^+, the vortices of significance with respect to the mean vorticity distribution are those of height $h^+ \approx O(y^+)$. It is interesting to note that, in Ref. [18], a functional form of $\partial \langle u^+ \rangle / \partial y^+$ has been suggested, and it is based upon an analysis in which hairpin vortices are assumed to undergo plane straining while growing from some initial height ($0.5\ \delta_o^+$) to a supposed final height (δ_o^+). Without actually invoking the Biot-Savart integral to calculate the associated induced field, the conjectured $\partial \langle u^+ \rangle / \partial y^+$ has the following form:

$$\frac{\partial \langle u^+ \rangle}{\partial y^+} = \begin{cases} \frac{1}{\kappa} \frac{1}{\delta_o^+} & , \ y^+/\delta_o^+ < 0.5 \\ \frac{1}{\kappa} \left(\frac{1}{y^+} - \frac{1}{\delta_o^+} \right) & , \ 0.5 \leq y^+/\delta_o^+ \leq 1.0 \\ 0 & , \ y^+/\delta_o^+ > 1.0 \end{cases} \tag{37}$$

where κ is the von Karman constant and δ_o^+ is a constant for the vortex under consideration. The distribution given by Eq. (37) looks quite similar in its general behavior to the distribution depicted in Fig. 11(b) which may be approximated by Eq. (36).

The main features of the proposed hairpin vortex model have been discussed in detail. The representative vortices of various sizes are assumed to be geometrically similar and have the same characteristic velocity scale. In addition, these vortices are considered as temporarily frozen while being convected toward downstream at constant mean velocities. The convection velocity of a representative vortex is defined as the mean flow velocity measured at some particular ground fixed point, at which the averaged contribution of this vortex to the mean flow velocity vanishes. This point is quite close to the tip of the vortex, consequently, larger vortices have higher mean convection velocity. In other words, the smaller vortices are convected back relative to the larger vortices and the largest vortices are convected back relative to the free stream. Based on this model of hairpin vortices, a statistical model of wall turbulence can be constructed.

A STATISTICAL MODEL OF TURBULENT BOUNDARY LAYER

Aspects of the Statistical Model

The wall region of the turbulent boundary layer is considered as consisting of trains of arrays of slanted hairpin vortices which are attached to the wall and convected toward the downstream. As indicated before, the effects of an array of vortices can be represented by those of a representative hairpin vortex. The representative vortex is inclined to the wall at an angle of 45° toward downstream direction. The effective centerline of the representative vortex has the shape of an isosceles triangle and it also has a slender viscous core. The representative vortex is considered at the present time as temporarily frozen while carried by its surroundings with a constant mean convection velocity. Representative vortices of the same size have the same structure and they are spaced, in average, with constant distance in the streamwise direction, but their lateral positions are random with respect to each other. Representative vortices of different sizes are assumed to be geometrically similar yet have the same characteristic velocity scale. The geometrical similarity applies to all length scales including the streamwise spacing. However, in addition to the randomness of their relative positions in the lateral direction, the streamwise positions of the representative vortices of different sizes also are random with respect to each other. It is noted here that the baseline vortex, i.e., the smallest hairpin vortex arises in the logarithmic law region, has length scales comparable with the Kline scalings. It is also clear that, in the present model of hairpin vortices, the height of a representative vortex determines all its other length scales, therefore, it is chosen as the primary parameter for describing the characteristics of the vortices.

It is assumed here that all the representative vortices are statistically independent and they do not interact strongly with each other. Consequently, any effects due to the interactions between representative vortices are neglected when compared with the self induction effects of individual vortices, and the instantaneous total flow field is simply a superposition of the induced flow fields associated with individual vortices whose relative arrangement is random. It is on this basis that the height of the vortices can be considered as the independent, random variable so that various statistical quantities of the wall turbulence are obtained from properly combining the contributions due to individual, representative hairpin vortices.

Imagine that there exists a sampling plane slanting at an angle of 45°, and over a sufficiently long period of time, an ensemble of representative hairpin vortices of various heights have been collected. Let the range of the height be $[h_{min}, h_{max}]$ and $\rho(h)$ be the probability density function of the independent random variable h. Then, for any real single-valued continuous function g(h), its expected mean value is given by [28]

$$\bar{g} = \int_{h_{min}}^{h_{max}} g(h)\,\rho(h)\,dh \tag{38}$$

where g can be velocity, pressure or any derived quantities such as the Reynolds stresses and other correlations.

This ensemble of representative hairpin vortices are now classified into N hierarchies or groups according to the vortex height. A representative vortex is considered to be in the ith hierarchy, if its height h falls inside the range $h_i - \Delta h/2 \leq h \leq h_i + \Delta h/2$, where h_i is the characteristic scale of the ith hierarchy and Δh is the range of the hierarchy. Consequently

$$\bar{g} = \sum_{i=1}^{N} \int_{h_i - \Delta h/2}^{h_i + \Delta h/2} g(h)\,\rho(h)\,dh \tag{39}$$

where $h_i = h_{min} + (i-1/2)\Delta h$ and $\Delta h = (h_{max} - h_{min})/N$.

For each hierarchy

$$\int_{h_i - \Delta h/2}^{h_i + \Delta h/2} g(h)\,\rho(h)\,dh = g_{si}\int_{h_i - \Delta h/2}^{h_i + \Delta h/2} \rho(h)\,dh = g_{si}P_i \tag{40}$$

where g_{si} is on averaged contribution of vortices within the ith hierarchy to the expected mean value and P_i is the probability distribution function of the ith hierarchy, i.e., it is the probability that a vortex will have its height falling inside the range $h_i - \Delta h/2 \leq h \leq h_i + \Delta h/2$. For sufficiently small Δh, g_{si} is approximated here by the averaged contribution of a typical vortex ($h = h_i$) to the expected mean value, i.e.

$$\bar{g} = \sum_{i=1}^{N} \langle g(h_i) \rangle P_i \tag{41}$$

In particular, if $\bar{g}$ is evaluated at different vertical locations, the above equation has the following form:

$$\bar{g}(y) = \sum_{i=1}^{N} \langle g(y; h_i) \rangle P_i \tag{42}$$

Since the averaged contribution to any flow quantity due to a typical vortex of height h_i can be evaluated (see, e.g. Eqs. (34) and (35)), the expected mean value due to an ensemble of hierarchies of vortices can be obtained, if the probability distribution among the hierarchies is known. In the present work, P_i is determined by matching the measured mean flow vorticity to the expected mean value of spanwise vorticity as obtained by the above synthesis procedure. The match is carried out in the least-squares sense. Subsequently, the distribution of any other statistical quantity among the hierarchies of representative hairpin vortices follows directly from the probability distribution needed to give the measured mean flow vorticity.

Thus, the turbulent boundary layer is considered as consisting of an ensemble of hierarchies of representative hairpin vortices. Each hierarchy of vortices is further approximated by a typical vortex whose height is the characteristic scale of the hierarchy under consideration. As indicated in the previous section (see Eq. (24)), the specific value of the strength factor C needs to be determined. This factor is a constant for a given ensemble of hierarchies of vortices and it yields the absolute strength of the typical vortices involved in a given ensemble of vortex hierarchies used to represent

the turbulent boundary layer. This factor C is easily determined by applying a fundamental property of P_i, namely,

$$\sum_{i=1}^{N} P_i = 1 \tag{43}$$

Another important quantity involved in the present statistical model is the convection velocity of the typical vortex. It is presumed to be the mean flow velocity measured at some particular ground fixed point, at which the averaged contribution of the typical vortex under consideration to the mean flow vanishes. However, when this presumed convection velocity is reciprocally used in the proposed synthesis procedure to determine the expected mean flow velocities at other points, there is no guarantee that the expected mean profile will automatically match the measured mean profile. Thus, such a presumed convection velocity needs to be validated by comparing the expected mean flow velocity profile with the actually measured mean velocity profile.

Obviously, the application of the present procedure requires the knowledge of the measured mean flow velocity $U_m(y)$. By simulating the wall turbulence with an ensemble of N typical, representative hairpin vortices of different heights, the expected mean vorticity is given by

$$\frac{\partial \bar{u}}{\partial y} = \sum_{i=1}^{N} P_i \frac{\partial \langle u \rangle_i}{\partial y} \tag{44}$$

At first, a tentative probability distribution is obtained by minimizing

$$\epsilon^2 = \sum_{j=1}^{M} \epsilon_j^2 \qquad (M \geq N) \tag{45}$$

where

$$\epsilon_j = \frac{\partial \bar{u}}{\partial y}(y_j) - \frac{\partial U_m}{\partial y}(y_j) \tag{46}$$

Then, the normalized probability distribution P_i and the strength factor C are simultaneously determined by imposing the condition given by Eq. (43). On the other hand, the vertical point y_{*i}, at which the averaged streamwise induced velocity of the ith vortex vanishes (see Fig. 11(a)), can be independently located, and the convection velocity of the ith vortex is given by

$$q_i = U_m(y_{*i}) \tag{47}$$

As mentioned above, q_i must be validated by comparing $U_m(y)$ with $\bar{u}(y)$, where

$$\bar{u}(y) = \sum_{i=1}^{N} P_i \langle u(y) \rangle_i \tag{48}$$

and $\langle u(y) \rangle$ is defined in Eq. (34) which, among other quantities, includes q.

The probability distribution among hierarchies and the factor needed to determine the absolute strength of vortices are now available. After the validation of the presumed convection velocities, various statistical quantities of the wall turbulence can be predicted by using Eq. (42). This implies that the distribution of any statistical quantity among the hierarchy scales follows directly from the probability distribution needed to give the measured mean flow vorticity. It is certainly possible to determine P_i by considering other statistical quantities, however, the mean flow velocity, or equivalently, the mean flow vorticity is the most convenient one to be measured or calculated, therefore, it is chosen for this initial effort.

Preliminary Assessment of the Statistical Model

At the present stage of development, the proposed hairpin vortex model is considered as most pertinent to the logarithmic law region of the turbulent boundary layer. Therefore, a preliminary assessment of the general behavior of this model is carried out for this region. The mean velocity profile in this region is given by (see e.g. [29])

$$U_m^+(y^+) = \frac{1}{0.4} \ln y^+ + 5.0, \quad 100 \leq y^+ \leq 500 \tag{49}$$

Different ensembles of representative hairpin vortices are used to simulate the wall turbulence in this region. Their heights fall inside the range $100 \leq h^+ \leq 500$. The probability distribution among vortices of each ensemble is determined by matching the expected mean vorticity obtained with Eq. (43) and Eq. (44) to the known mean vorticity derived from Eq. (49). The matching procedure is carried out for N vortices and M vertical points in the least-squares sense. Before specific results are presented, several comments on the matching procedure need to be made.

When Δh the difference of height between the typical vortices becomes smaller, the solution matrix associated with the matching procedure tends to be singular. This is not surprising, because nearly identical vortices are used so that the differences of the coefficients between neighboring rows of the solution matrix are quite small. Thus, there exists a practical lower limit of Δh. On the other hand, if Δh becomes sufficiently large, important length scales which are physically occurring in the region of interest cannot be satisfactorily accounted for by these vortices. Apparently, in practice there exists an optimum range of Δh. Further, as mentioned in the previous section (also see Fig. 14), at level y, the vortices of significance with respect to the mean vorticity distribution are those of height $h = O(y)$. Consequently, the absence of the vortices of $h^+ < 100$ or those of $h^+ > 500$ will not significantly affect the probability distributions of vortices whose heights fall between, say, $100 \leq y^+ \leq 400$. However, the absence of vortices of heights $h^+ > 500$ will significantly affect the probability distributions of the vortices whose heights are close to $y^+ \approx 500$. In other words, the effects of those absent larger vortices are expected to be accounted for by increased probability distributions of the vortices of $h^+ = O(500)$. Therefore, the solution of probability distributions of vortices whose heights are larger than $y^+ = 400$ should be interpreted carefully. In addition, the points, at which the matching procedure is carried out, are chosen to be in the range $100 \leq y^+ \leq 400$.

The results obtained for four different ensembles of typical hairpin vortices are now presented. In all of these cases, the matching procedure is performed at 37 points (M=37), their positions range from $y^+ = 97$ to $y^+ = 395$ with $\Delta y^+ = 8.1$. The arrangement of these ensembles of vortices as well as the calculated strength factor C are given in Table I.

Table I - Demonstration Cases

CASE	N	h^+_{min}	h^+_{max}	Δh^+	C
1	9	100	500	50	2.835
2	8	125	475	50	2.572
3	6	125	500	75	2.667
4	6	100	475	75	2.846

The probability distribution among hierarchies of vortices is illustrated in Fig. 15. As discussed before, the predicted probability distributions of vortices with $h^+ \geq 400$ should be considered here as larger than their true values, because the effects of absent larger vortices on the mean flow vorticity in the region of $y^+ \geq 400$ are mainly accounted for by those introduced vortices of $400 \leq h^+ \leq 500$. A correlation analysis indicates that, for vortices of heights between $y^+ = 100$ and $y^+ = 350$, there is a strong linear correlation between height and probability distribution of vortices (Fig. 15). The linear correlation is expressed as

$$P = 0.01\, mh^+ + b \tag{50}$$

The values of m, b are given in Table II, in which r is the linear correlation coefficient and r_d is the decision point for the strength of the linear correlation. A linear correlation is considered as existing if $|r| \geq r_d$.

Table II - The Linear Correlation Between P and h^+

CASE	m	b	r	r_d
1	-0.049	0.198	-0.952	0.811
2	-0.051	0.213	-0.926	0.811
3	-0.056	0.257	-0.971	0.95
4	-0.080	0.295	-0.960	0.95

Obviously, in the region of $100 \leq y^+ \leq 350$, the probability distribution of a typical hairpin vortex decreases when its height increases. This is consistent with the general behavior of the probability distribution of hierarchies discussed in Ref. [18].

Figure 16 shows the convection velocity as a function of the vortex height, it indicates that larger vortices are convected at higher velocities. The free stream velocity $\bar{u}_e^+$ is usually of the order of 30, therefore, the mean convection velocities of these vortices are in the range $0.55 \leq q^+/\bar{u}_e^+ \leq 0.68$. They are consistent with observed values associated with the large scale structures in the wall region. As mentioned before, these presumed convection velocities must be validated by comparing the expected values of mean flow velocity profile predicted by Eq. (48) with the known distribution given by Eq. (49). The comparisons indicate that, for the four cases considered, the relative errors are uniformly less than 6%. In addition, from Tables I, II as well as Fig. 15, it can be seen that the results are relatively insensitive to the number of hierarchies used in simulating the wall turbulence.

The main features of the fluctuating as well as averaged flow fields associated with individual representative hairpin vortices have been discussed in the previous section, the general behavior of the probability distributions and the convection velocities of typical vortices in an ensemble of hairpin vortices simulating the wall turbulence are briefly assessed in the present section. These results suggest that the use of hairpin vortex in obtaining a quantitative link between the mean flow, Reynolds stresses and other correlations in wall turbulence looks promising. The ultimate justification of applying the proposed model of wall turbulence to turbulent boundary layer flows depends on the success with which it can be used to predict various turbulence quantities. Such a detailed assessment should be carried out in the future.

CONCLUDING REMARKS

Predictions of the far-field trailing edge noise require as input the space-time correlations of incident surface pressure fluctuations, which are obtained to date mainly by extensive measurements. The goal of the present effort is to develop a theoretical technique to estimate these pertinent data by considering the hairpin vortex as the underlying structure of the wall turbulence and by using the hairpin vortex to provide a quantitative link between the mean flow and various turbulence quantities. A mathematically operational model of the hairpin vortex is developed, and the main features of such a model has been discussed in detail. The turbulent boundary layer is considered as consisting of an ensemble of representative hairpin vortices of different length scales, i.e., hierarchies of typical hairpin vortices. A synthesis technique is developed to determine the strengths, convection velocities as well as the probability distributions of these typical vortices. Further, the distribution of any turbulence quantity (including the space-time correlation of the fluctuating pressure field) among the hierarchies of typical vortices follows directly from the probability distribution needed to give the measured mean vorticity profile. At the present stage of the development of the synthesis technique, the proposed hairpin vortex model of wall turbulence is considered as most pertinent to the logarithmic law region of the turbulent boundary layer. Preliminary results obtained in this region indicate that the application of the synthesis technique to estimate the aerodynamic input via hairpin vortex model of turbulent boundary layer for use in trailing edge noise prediction theories is quite feasible.

It is obvious that the applicability of the present approach should be assessed in a more detailed fashion. For example, the predicted Reynolds shear stress as well as the turbulence intensities should be compared with measured data. The model of hairpin vortex should also be modified to properly simulate the flow structures occurring in the viscous sublayer, buffer zone as well as the outer wake region. For a decelerated turbulent boundary layer flow, the effects of adverse pressure gradient should also be included by suitably modelling the structures arising in the half power law region. Finally, it is of great interest to develop the capability for investigating the dynamic behavior of hairpin vortices submerged in various background flows by numerical simulation through the solution of unsteady, three-dimensional Navier-Stokes

equations. The dynamic information obtained will greatly enhance the understanding of the deterministic turbulent structures per se and, therefore, can be used to construct improved vortex model of turbulent boundary layer flows.

REFERENCES

1. Brooks, T.F., and Schlinker, R.H.: Progress in Rotor Broadband Noise Research, Vertica Vol. 7, No. 4, pp. 287-307, 1983.

2. Brooks, T.F., and Hodgson, T.H.: Trailing Edge Noise Prediction From Measured Surface Pressures, J. of Sound and Vibration, Vol. 78, No. 1, pp. 69-117, 1981.

3. Yu, J.C. and Joshi, M.C.: On Sound Radiation From the Trailing Edge of an Isolated Airfoil in a Uniform Flow, AIAA Paper No. 79-0603, 1979.

4. Howe, M.S.: A Review of the Theory of Trailing Edge Noise, J. of Sound and Vibration, Vol. 61, pp. 437-465, 1978.

5. Amiet, R.K.: Effect of the Incident Surface Pressure Field on Noise Due to Turbulent Flow Past a Trailing Edge, J. of Sound and Vibration, Vol. 57, pp. 305-306, 1978.

6. Willmarth, W.W.: Pressure Fluctuations Beneath Turbulent Boundary Layers, Annual Review of Fluid Mech., pp. 13-38, 1975.

7. Landahl, M.T.: A Wave-Guide Model for Turbulent Shear Flow, J. of Fluid Mech. Vol. 29, Part 3, pp. 441-459, 1967.

8. Reynolds, W.C. and Hussain, A.K.M.F.: The Mechanics of an Organized Wave in Turbulent Shear Flow, Part 3, Theoretical Models and Comparison with Experiments, J. Fluid Mech., Vol. 54, Part 2, pp. 263-288, 1972.

9. Theodorsen, T.: The Structure of Turbulence, 50 Jahre Grenzschichtforschung, ed. H. Gortler & W. Tollmien, p. 55, Braunschweig: Veiweg und Sohn. 1955.

10. Black, T.J.: Some Practical Applications of a New Theory for Wall Turbulence, Proc. 1966 Heat Transfer and Fluid Mech. Inst., Stanford University Press, 1966.

11. Head, M.R. and Bandyopadhyay, P.: New Aspects of Turbulent Boundary-Layer Structure, J. Fluid Mech. Vol. 107, pp. 297-338, 1981.

12. Falco, R.E.: A Synthesis and Model of Turbulence Structure in the Wall Region, Structure of Turbulence in Heat and Mass Transfer, ed. Z.P. Zaric, pp. 43-57, 1982, Hemisphere Publishing Corp.

13. Dinkelacker, A.: Do Tornado-Like Vortices Play a Role in Turbulent Mixing Processes? Structure of Turbulence in Heat and Mass Transfer, ed. Z.P. Zaric, pp. 59-72, 1982. Hemisphere Publishing Corp.

14. Viets, H., Bethke, R.J. and Bougine, D.: Three-Dimensional Vortex Dynamics Near a Wall, Fourth International Symposium on Turbulent Shear Flow, Karlsruhe, West Germany, 1983.

15. Moin, P. and Kim, J.: Structure of the Vorticity Field in Turbulent Channel Flow, Part I: Analysis of Instantaneous Fields and Statistical Correlations, NASA TM-86019, 1984.

16. Landahl, M.T.: Coherent Structures in Turbulence and Prandtl's Mixing Length Theory, Z. Flugwiss, Weltraumforsch. 8, pp. 233-242, 1984.

17. Townsend, A.A.: The Structure of Turbulent Shear Flow, 2nd edn. Cambridge University Press, 1976.

18. Perry, A.E. and Chong, M.S.: On the Mechanism of Wall Turbulence, J. Fluid Mech., Vol. 119, pp. 173-217, 1982.

19. Perry, A.E., Henbest, S.M. and Chong, M.S.: Further Spectral Analysis of Smoothed-Wall Pipe Flow, Fourth International Symposium on Turbulent Shear Flow, Karlsruhe, West Germany, 1983.

20. Leonard, A.: Vortex Methods for Flow Simulation, J. of Comput. Physics, Vol. 37, pp. 289-335, 1980.

21. Weinberg, B.C., McDonald, H. and Shamroth, S.J.: A Solution Procdure for Two and Three Dimensional Unsteady Flows, AIAA Paper 85-0298, 1985.

22. Ting, L.: Studies on the Motion and Decay of a Vortex Filament, Advances in Fluid Mechanics, Ed. E. Krause, pp. 67-105, 1980, Springer-Verlag.

23. Liu, N.-S., Shamroth, S.J. and McDonald, H.: Numerical Solution of the Navier-Stokes Equations for Compressible Turbulent Two/Three Dimensional Flows in the Terminal Shock Region of an Inlet/Diffuser, AIAA Paper 83-1892, July 1983.

24. Liu, N.-S., Shamroth, S.J. and McDonald, H.: Dynamic Response of Shock Waves in Transonic Diffuser and Supersonic Inlet: an Analysis with the Navier-Stokes Equations and Adaptive Grid, AIAA Paper 84-1609, June 1984.

25. Blackwelder, R.F.: The Bursting Process in Turbulent Boudary Layer, Proc. Workshop on Coherent Structure of Turbulent Boundary Layers, Lehigh University, p. 211, 1978.

26. Clark, J.A. and Markland, E.: Vortex Structures in Turbulent Boundary Layers, Aero. J. Vol. 74, pp. 243-244, 1970.

27. Lilley, G.M.: A Review of Pressure Fluctuations in Turbulent Boundary Layers at Subsonic and Supersonic Speeds, Arch. Mech. Stosow, 16:301, 1964.

28. Bendat, J.S. and Piersol, A.G.: Random Data: Analysis and Measurement Procedures, John Wiley & Sons, 1971.

29. Yaglom, A.M.: Similarity Laws for Constant-Pressure and Pressure-Gradient Turbulent Wall Flows. Ann. Rev. Fluid Mech., Vol. 11, pp. 505-540, 1979.

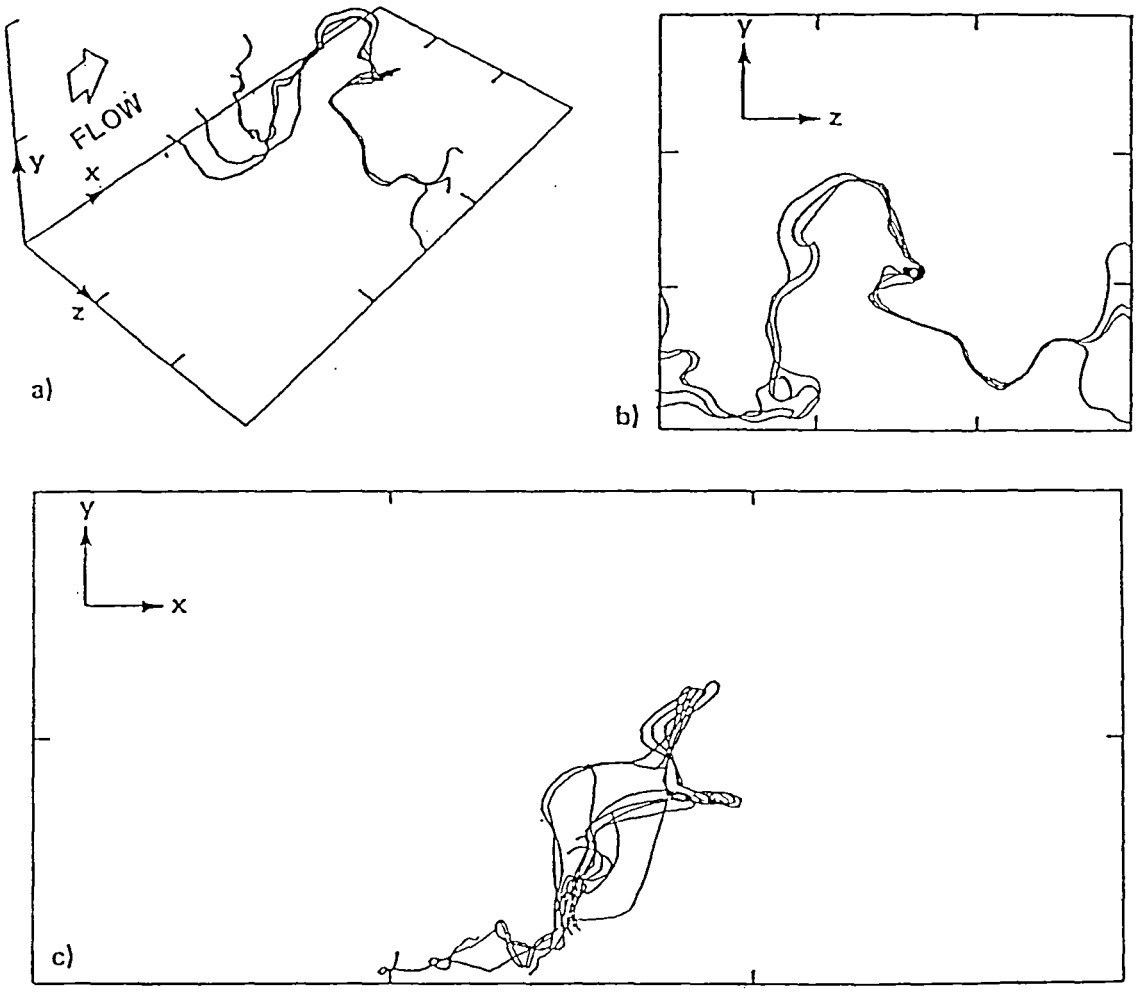

Figure 1. A set of vortex lines (vortex filament) resembling a hairpin-like structure. (a) 3-D view; (b) end-view; (c) side-view. The spanwise, z, extent of the figure is 700 υ/u_τ, the streamwise, x, extent of the figure is 1380 υ/u_τ. (From ref. 15)

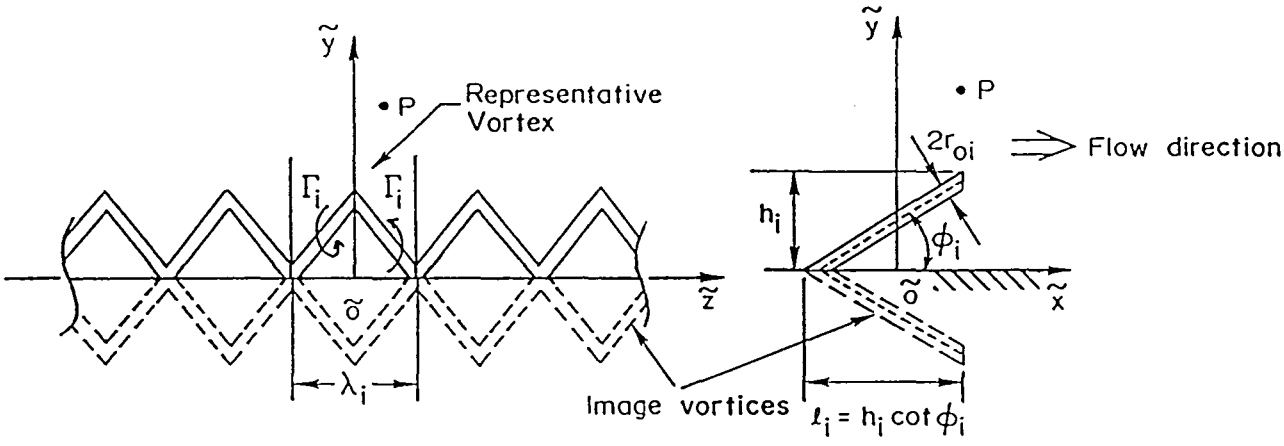

Figure 2. A schematic of an array of hairpin vortices and the representative vortex.

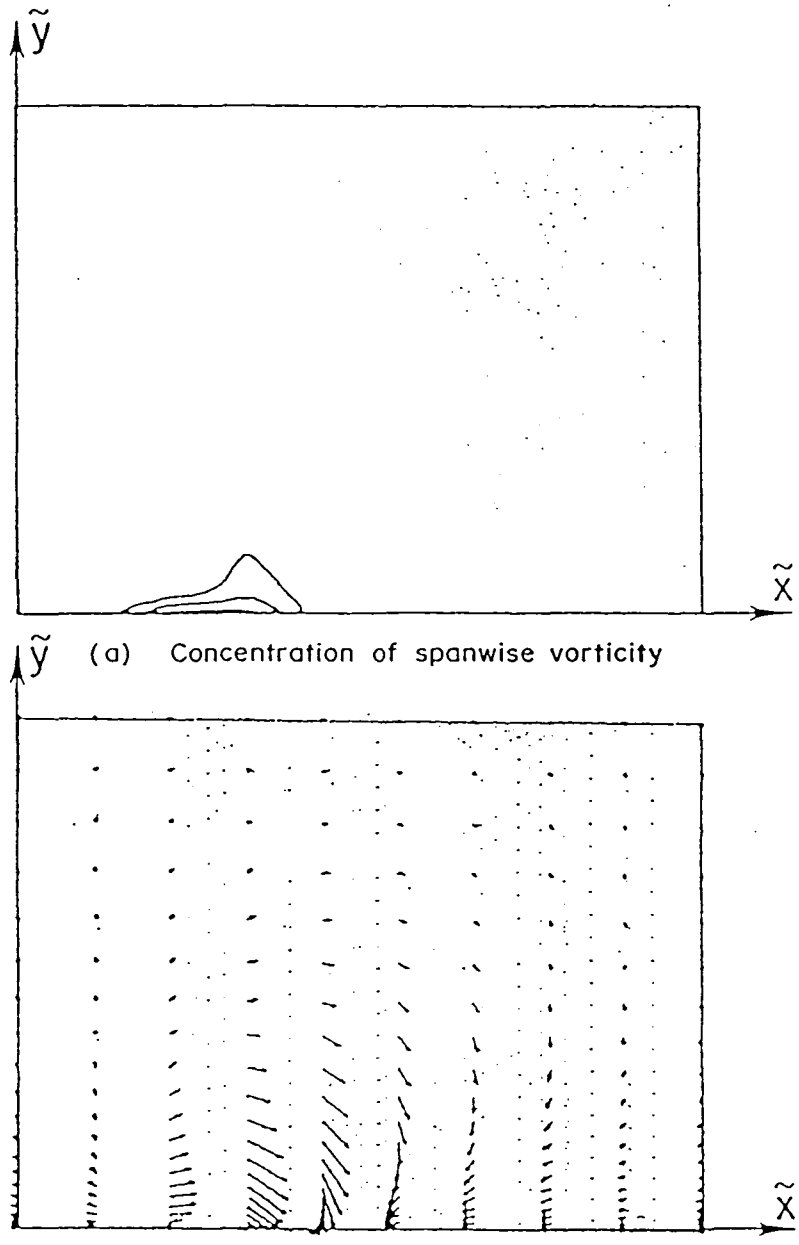

Figure 3. Flow pattern within a representative hairpin vortex in a plane parallel to the mean flow direction. The plane is at one foot of the vortex.

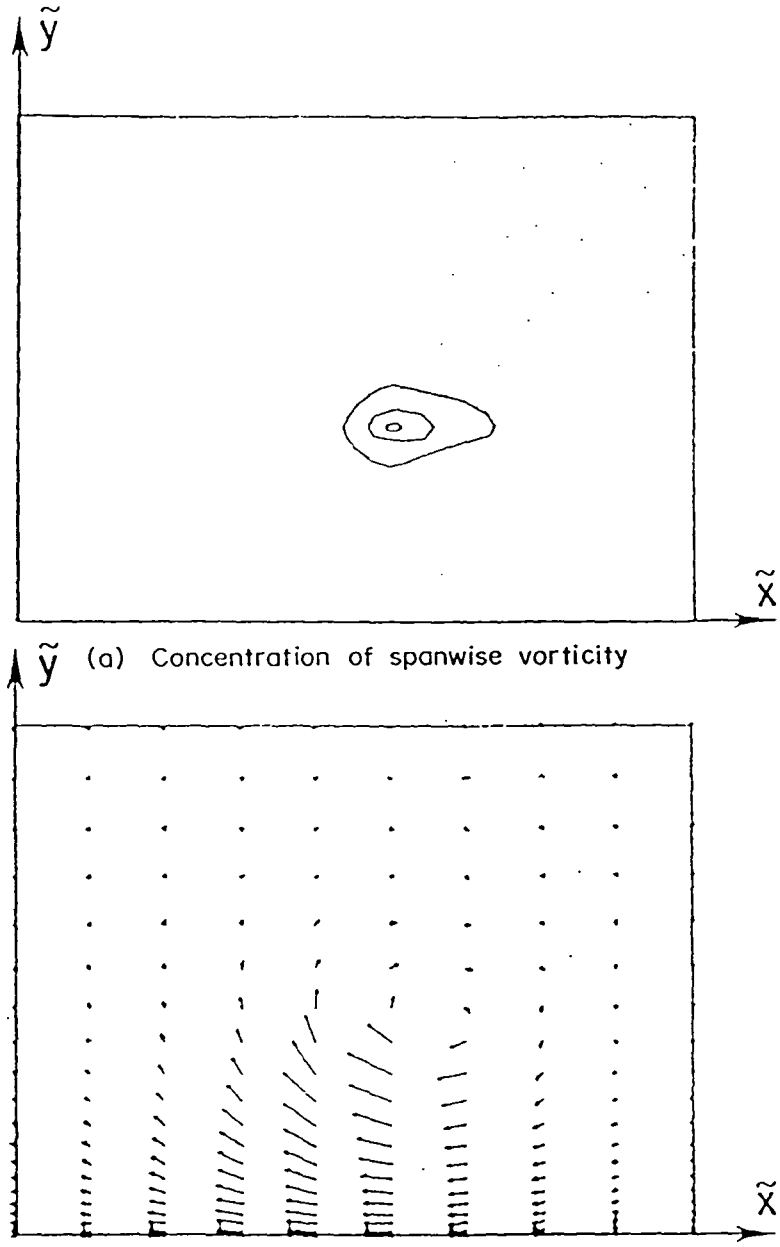

Figure 4. Flow pattern within a representative hairpin vortex in a plane parallel to the mean flow direction. The plane is at the tip of the vortex.

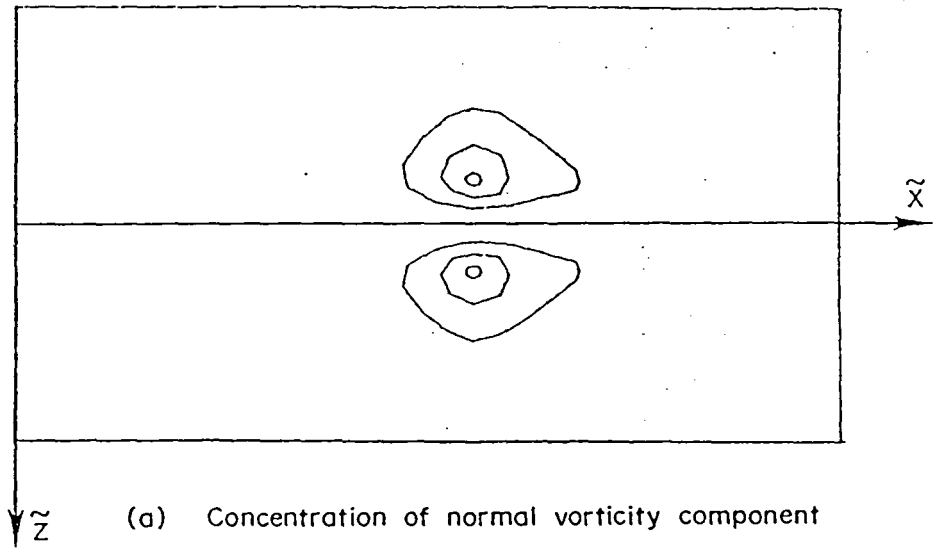

(a) Concentration of normal vorticity component

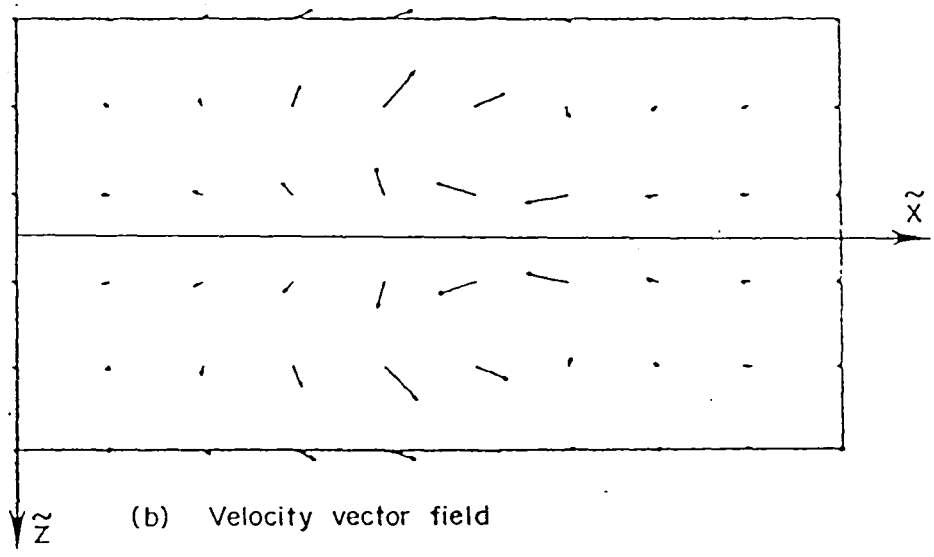

(b) Velocity vector field

Figure 5. Flow pattern within a representative hairpin vortex in a plane parallel to the flat wall. The plane is close to the tip of the vortex.

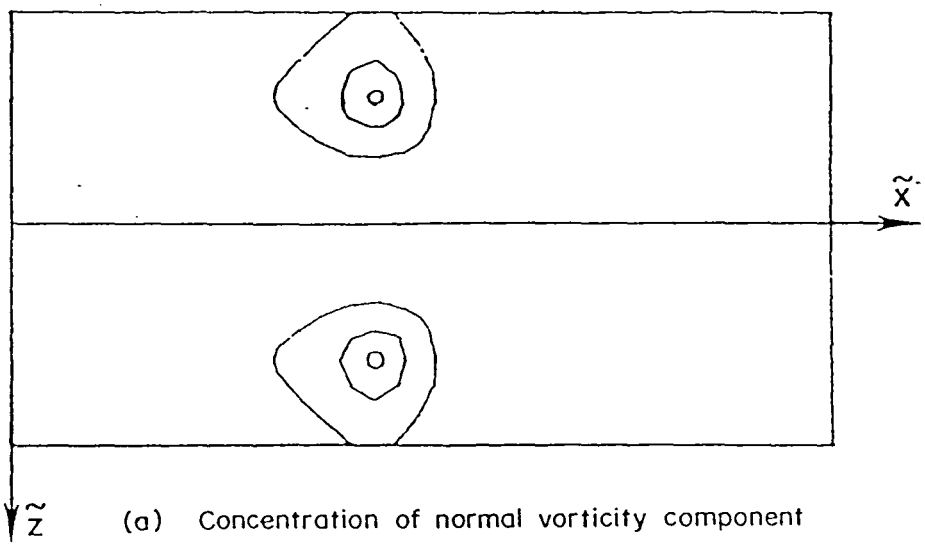

(a) Concentration of normal vorticity component

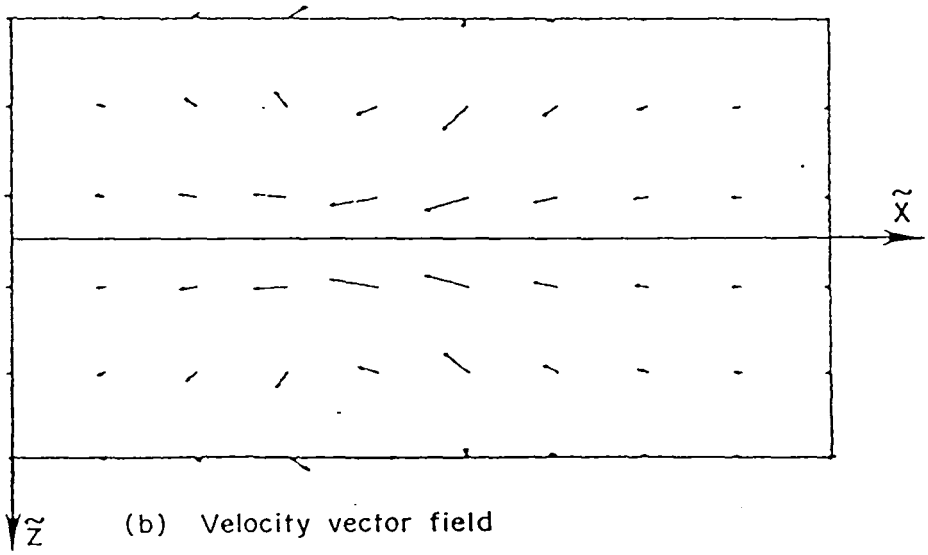

(b) Velocity vector field

Figure 6. Flow pattern within a representative hairpin vortex in a plane parallel to the flat wall. The plane is close to the wall.

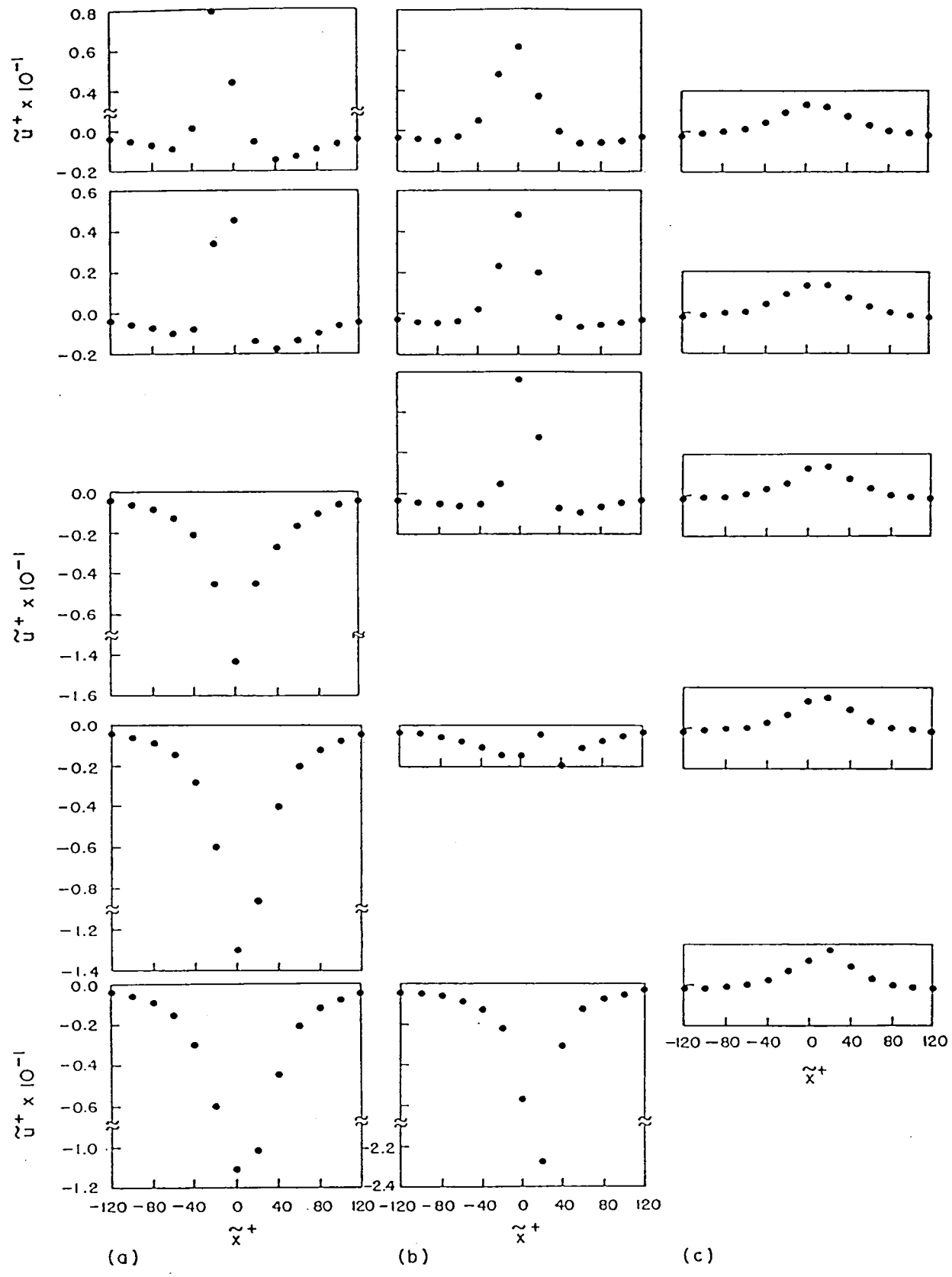

Figure 7. The induced field of the baseline hairpin vortex ($\tilde{u}^+ \times 10^{-1}$). Distributions are presented at three planes: (a) $y^+/h^+ = 0.4$, (b) $y^+/h^+ = 0.8$, (c) $y^+/h^+ = 1.6$. For each plane, five spanwise locations are selected to illustrate the variations. The five spanwise locations are (from top to bottom); $\tilde{z}^+/\lambda^+ = -0.5, -0.375, -0.25, -0.125, 0.0$. Note that $h^+ = 50$, $\lambda^+ = 100$.

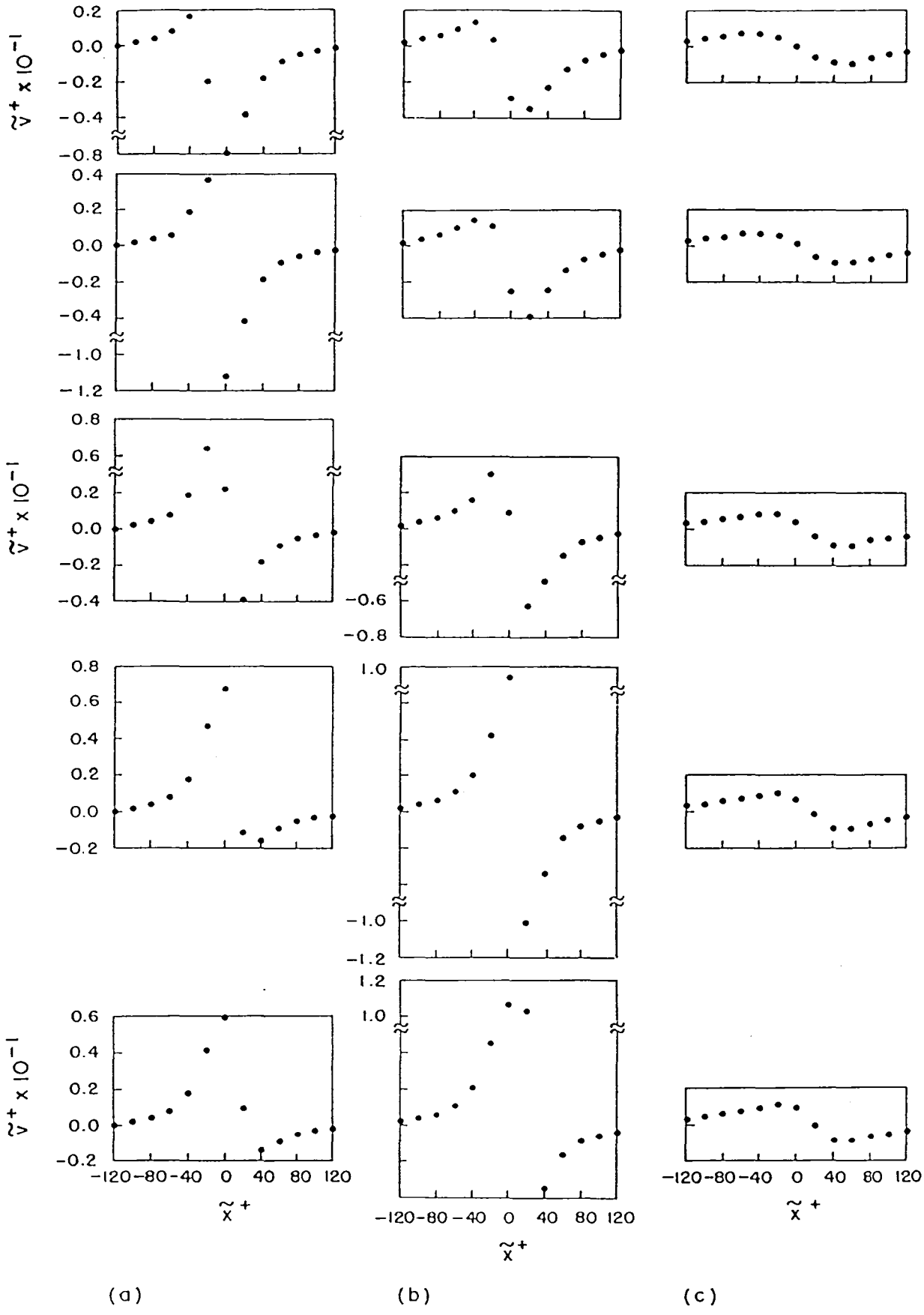

Figure 8. The induced field of the baseline hairpin vortex ($\tilde{v}^+ \times 10^{-1}$). See caption of Fig. 7 for details.

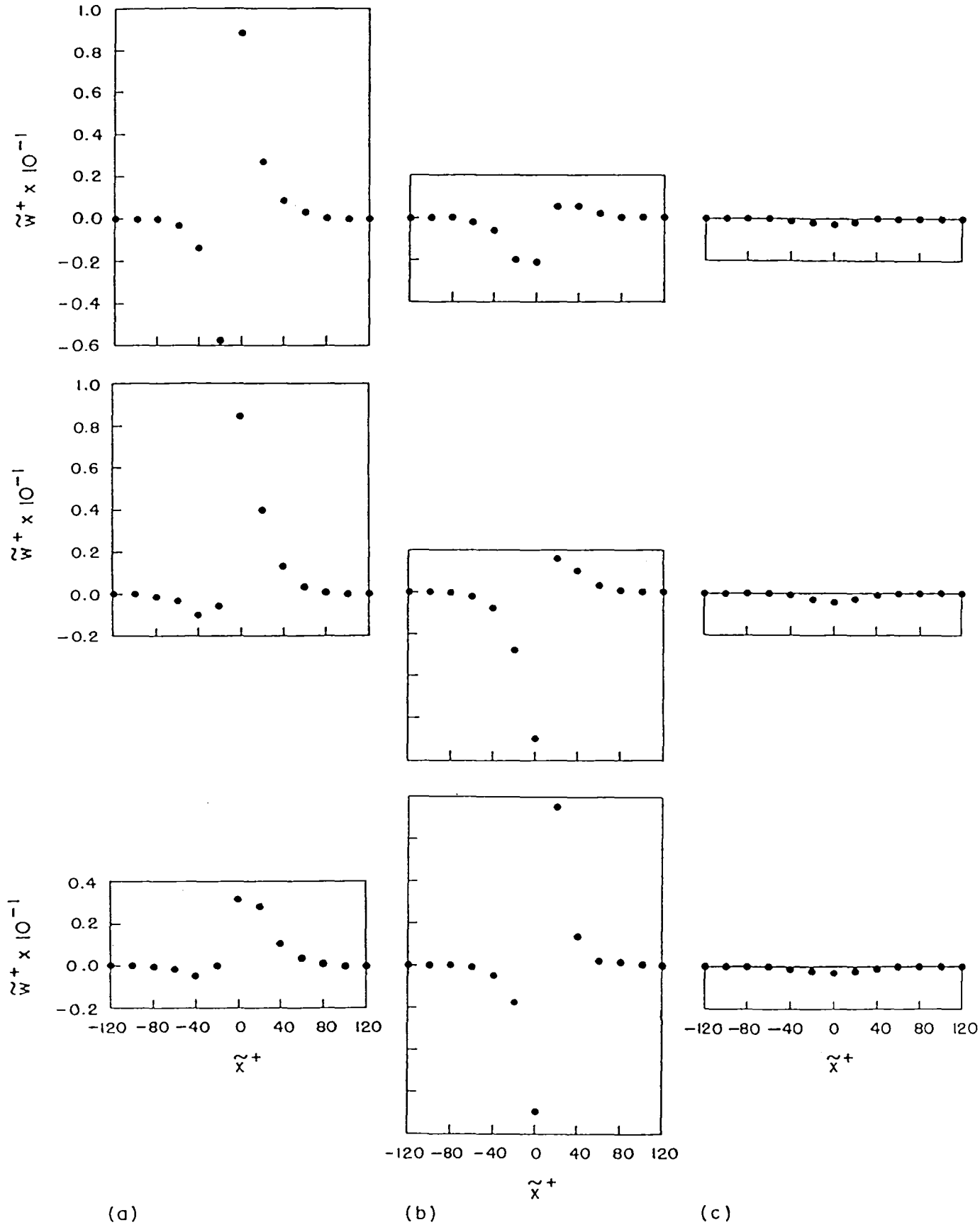

Figure 9. The induced field of the baseline hairpin vortex ($\tilde{w}^+ \times 10^{-1}$). See caption of Fig. 7 for details, except that $\tilde{w}^+$ values at $\tilde{z}^+/\lambda^+ = -0.5$ and 0.0 are zero and are not shown.

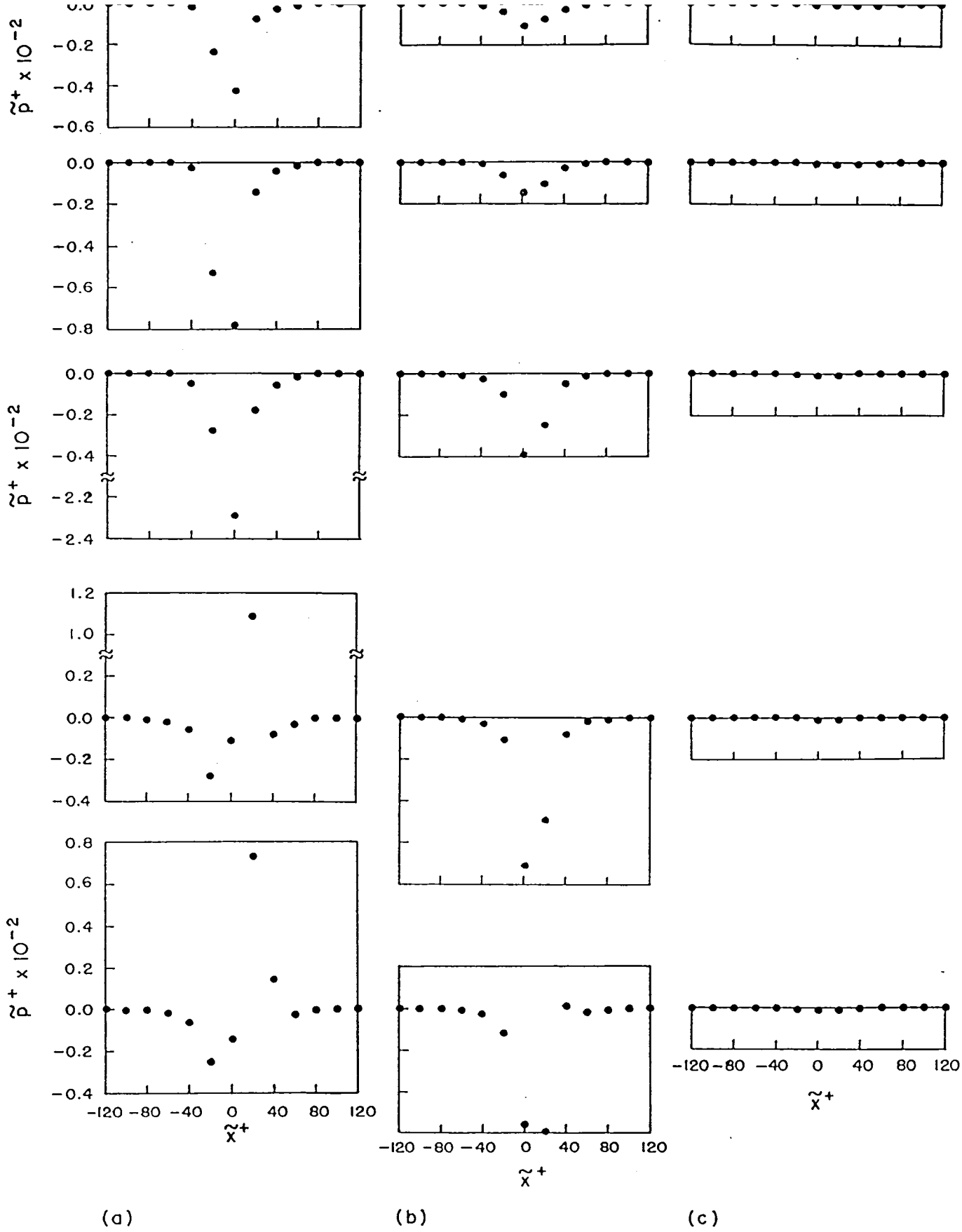

Figure 10. The induced field of the baseline hairpin vortex ($\tilde{p}^+ \times 10^{-2}$). See caption of Fig. 7 for details. Note that the induced pressure at $y^+ = 400 = 8h^+$ is considered as zero in the present case.

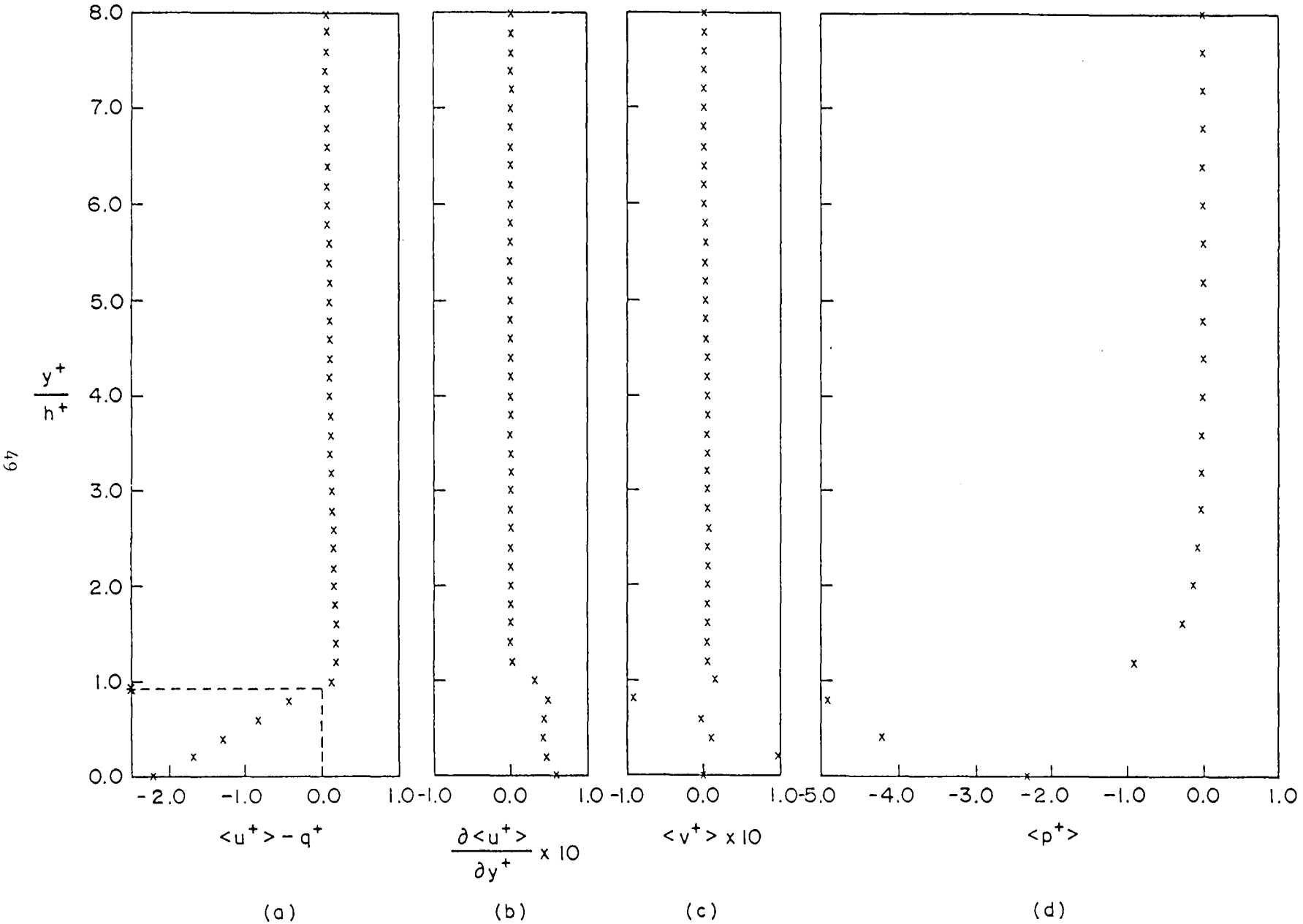

Figure 11. The mean field of the baseline vortex ($h^+ = 50$).

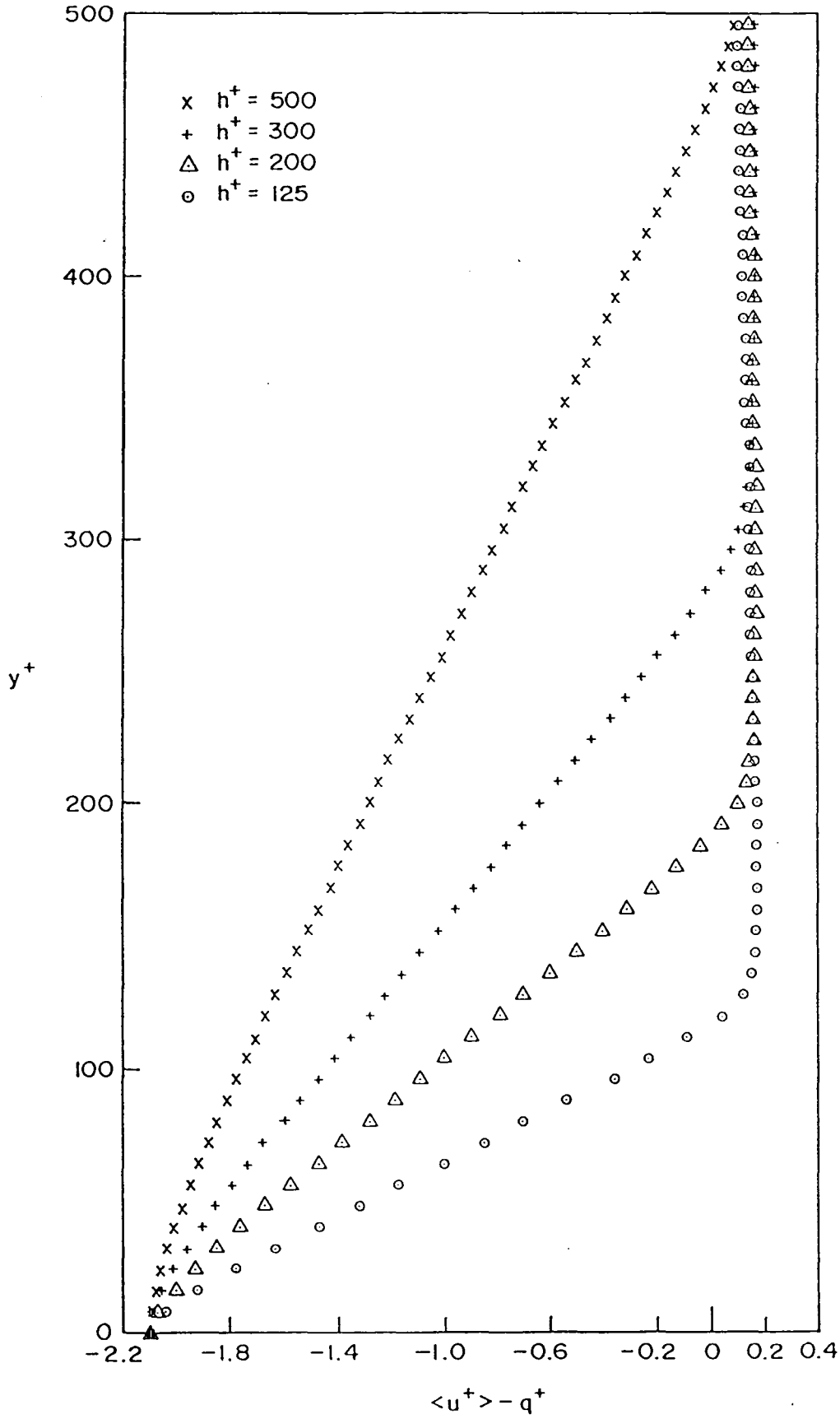

Figure 12. Averaged streamwise induced velocity due to hairpin votices of different sizes.

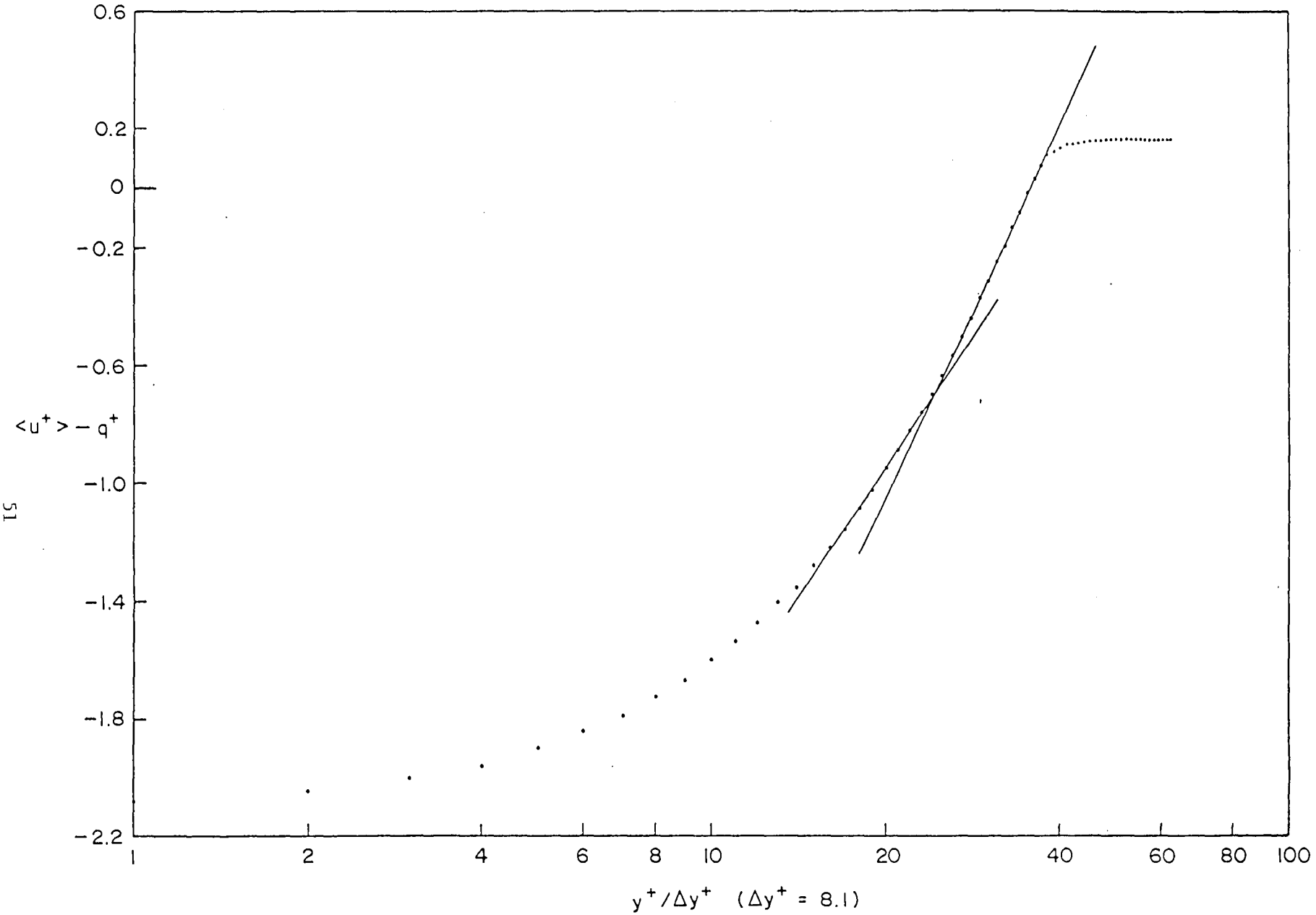

Figure 13. The averaged streamwise induced velocity of a hairpin vortex ($h^+ = 300$).

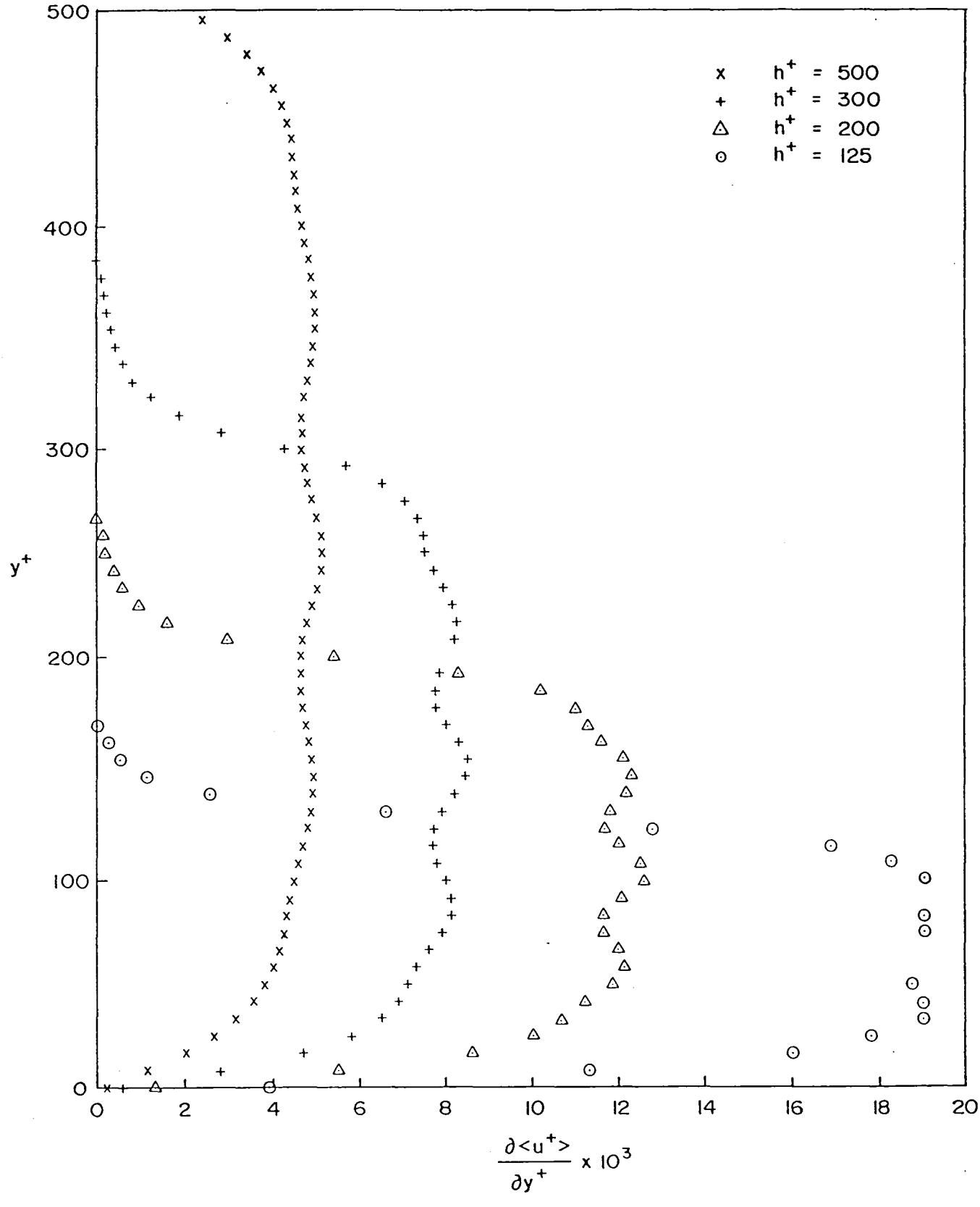

Figure 14. The averaged spanwise induced vorticity due to hairpin vortices of different sizes.

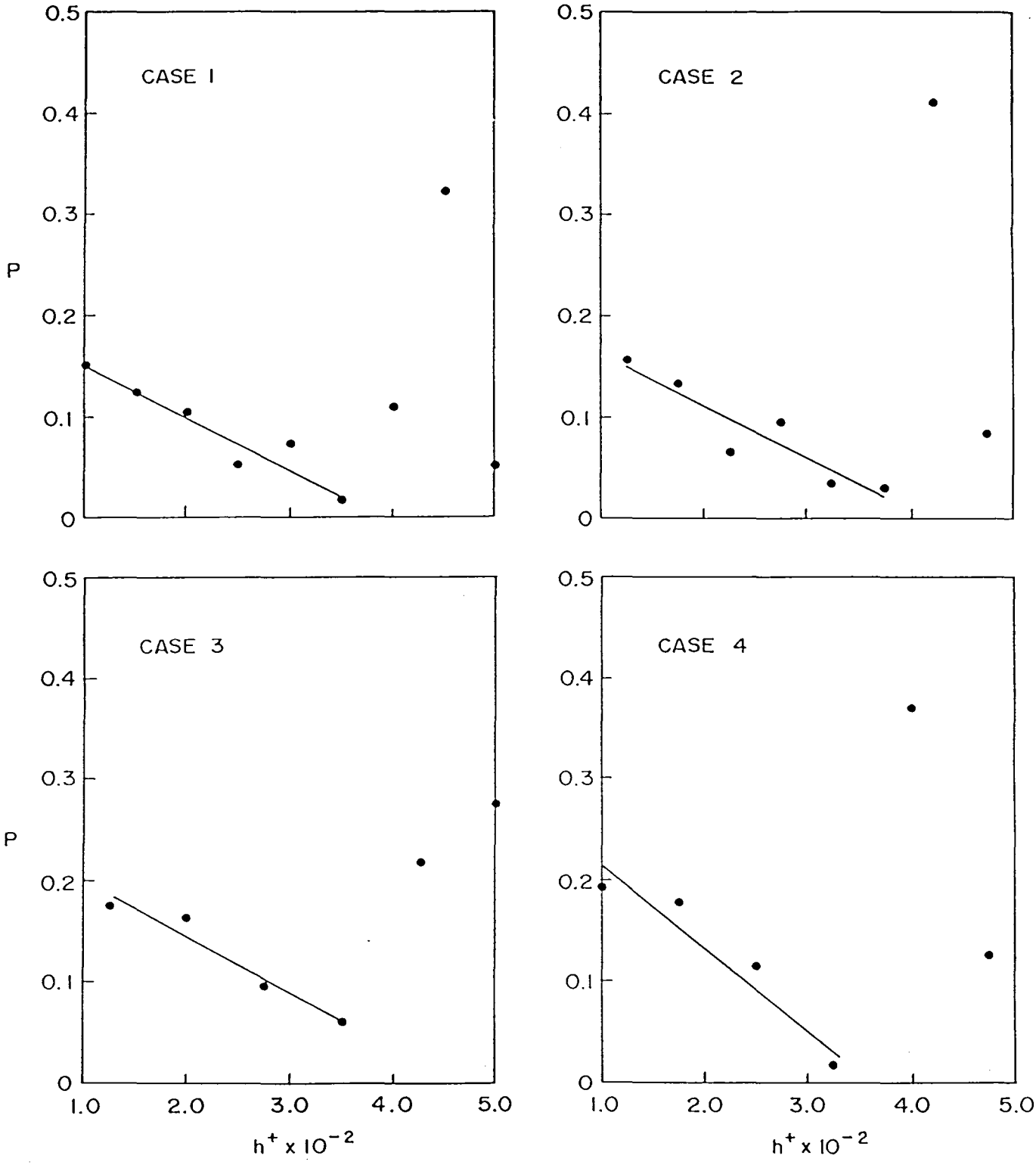

Figure 15. Probability distribution among hierarchies of typical vortices.

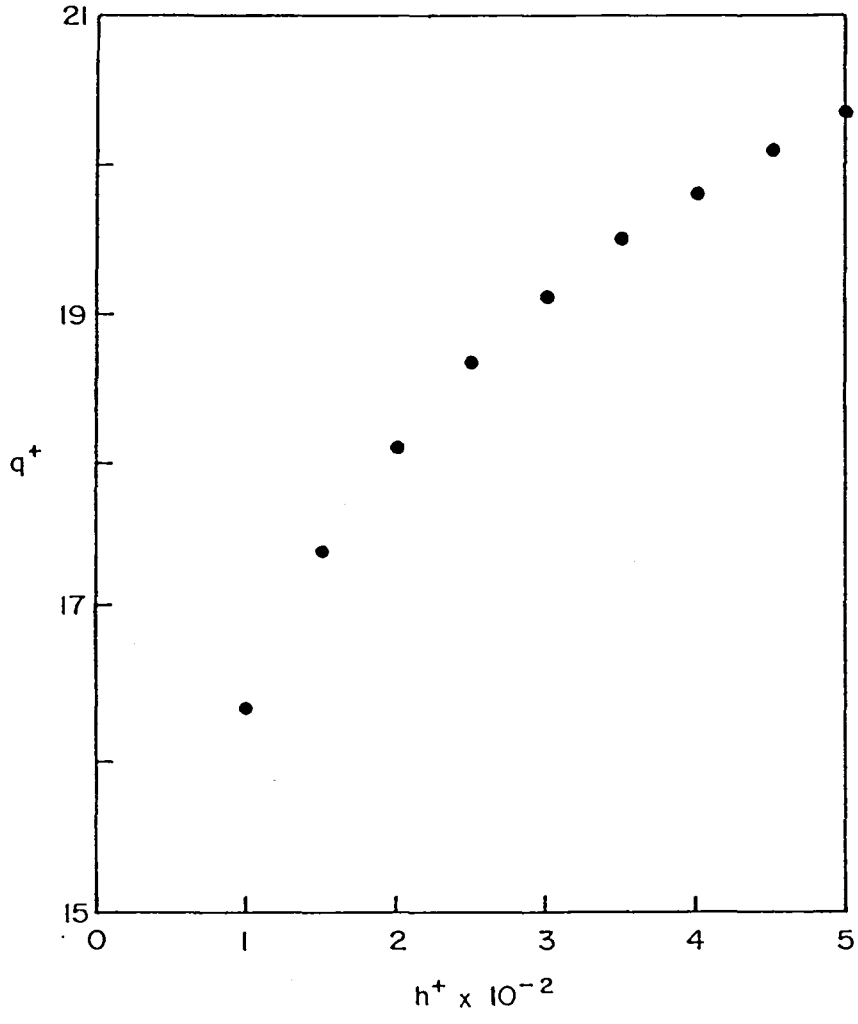

Figure 16. Convection velocities of typical hairpin vortices.

1. Report No.	2. Government Accession No.	3. Recipient's Catalog No.
NASA CR-177938		

4. Title and Subtitle	5. Report Date
ON THE APPLICATION OF A HAIRPIN VORTEX MODEL OF WALL TURBULENCE TO TRAILING EDGE NOISE PREDICTION	August 1985
	6. Performing Organization Code

7. Author(s)	8. Performing Organization Report No.
N.-S. Liu and S.J. Shamroth	R85-900026-F
	10. Work Unit No.

9. Performing Organization Name and Address	11. Contract or Grant No.
Scientific Research Associates, Inc. P.O. Box 498 Glastonbury, CT 06033	NAS1-17249
	13. Type of Report and Period Covered
12. Sponsoring Agency Name and Address	Contractor Report
National Aeronautics and Space Administration Washington, DC 20546	14. Sponsoring Agency Code

15. Supplementary Notes

Langley Technical Monitor: Thomas F. Brooks
Final Report

16. Abstract

The goal of the present work is to develop a technique via a hairpin vortex model of the turbulent boundary layer, which would lead to the estimation of the aerodynamic input for use in trailing edge noise prediction theories. The work described herein represents an initial step in reaching this goal. The hairpin vortex is considered as the underlying structure of the wall turbulence and the turbulent boundary layer is viewed as an ensemble of typical hairpin vortices of different sizes. A synthesis technique is examined which links the mean flow and various turbulence quantities via these typical vortices. The distribution of turbulence quantities among vortices of different scales follows directly from the probability distribution needed to give the measured mean flow vorticity. The main features of individual representative hairpin vortices are discussed in detail and a preliminary assessment of the synthesis approach is made.

17. Key Words (Suggested by Author(s))	18. Distribution Statement
Hairpin Vortices Synthesis Model of Turbulence	Unclassified - Unlimited

19. Security Classif. (of this report)	20. Security Classif. (of this page)	21. No. of Pages	22. Price
Unclassified	Unclassified	56	

N-305

For sale by the National Technical Information Service, Springfield, Virginia 22161

End of Document